Arbuscular Mycorrhizal Symbiosis Requires a Phosphate Transceptor in the Gigaspora margarita Fungal Symbiont

Arbuscular Mycorrhizal Symbiosis Requires a Phosphate Transceptor in the Gigaspora margarita Fungal Symbiont

Xianan Xie1, Hui Lin1, Xiaowei Peng1, Congrui Xu1, Zhongfeng Sun1, Kexin Jiang1, Antian Huang1, Xiaohui Wu1, Nianwu Tang1, Alessandra Salvioli2, Paola Bonfante2, Bin Zhao1

1 State Key Laboratory of Agricultural Microbiology, College of Life Science and Technology, Huazhong Agricultural University, Wuhan, Hubei 430070, P.R.China
2 Department of Life Sciences and Systems Biology, University of Torino, Viale Mattioli 25, 10125 Torino, Italy

Abstract

The majority of terrestrial vascular plants are capable of forming mutualistic associations with obligate biotrophic arbuscular mycorrhizal (AM) fungi from the phylum Glomeromycota. This mutualistic symbiosis provides carbohydrates to the fungus, and reciprocally improves plant phosphate uptake. AM fungal transporters can acquire phosphate from the soil through the hyphal networks. Nevertheless, the precise functions of AM fungal phosphate transporters, and whether they act as sensors or as nutrient transporters, in fungal signal transduction remain unclear. Here, we report a high-affinity phosphate transporter GigmPT from Gigaspora margarita that is required for AM symbiosis. Host-induced gene silencing of GigmPT hampers the development of G. margarita during AM symbiosis. Most importantly, GigmPT functions as a phosphate transceptor in G. margarita regarding the activation of the phosphate signaling pathway as well as the protein kinase A signaling cascade. Using the substituted-cysteine accessibility method, we identified residues A146 (in transmembrane domain [TMD] IV) and Val357 (in TMD VIII) of GigmPT, both of which are critical for phosphate signaling and transport in yeast during growth induction. Collectively, our results provide significant insights into the molecular functions of a phosphate transceptor from the AM fungus G. margarita.

Key words
mutualistic symbiosis; Gigaspora margarita; GigmPT; phosphate transceptor; phosphate signaling; protein kinase A

Introduction

Arbuscular mycorrhizal (AM) fungi are capable of establishing mutualistic symbioses with most terrestrial vascular plant species (Remy et al., 1994 and Harrison, 1999). These endosymbiotic associations between plants and AM fungi, namely arbuscular mycorrhizas, are widespread and ancient relationships in terrestrial ecosystems (Parniske, 2008). Since the obligate symbiotic AM fungi from the phylum Glomeromycota inhabit the soil and form associations with plant roots as part of their life cycle (Schüßler et al., 2001), AM fungi provide the mineral nutrients to the plants and in turn obtain carbohydrates (Smith and Read, 2008). Arbuscular mycorrhizas have an enormous effect on terrestrial ecosystems throughout the world (Smith and Smith, 1997). In general, AM symbiosis benefits plant growth and improves plant biodiversity and ecosystem productivity (van der Heijden et al., 1998).
Mycorrhizal plants can explore the soil substratum far from the depletion region through forming large hyphal networks for the uptake of nutrients (mainly phosphate) (Finlay, 2008 and Parniske, 2008). Within root cortical cells, symbiotic development results in the formation of arbuscules, differentiated hyphae in highly branched and tree-shaped structures that are considered to be the sites for nutrient exchange between the host and fungal partners (Parniske, 2008). Despite their great importance, the underlying molecular events driving the AM symbiosis and nutrient transfer remain only partially understood (Harrison, 2005, Paszkowski, 2006 and Bucher et al., 2009).
Although phosphate acquisition provides the key benefit for the plant, our understanding on the routes, mechanisms, and regulation of phosphate transport in AM symbiosis remains limited. Radiotracer studies demonstrated that the extraradical hyphae acquire phosphate, which is later translocated to the intraradical hyphae and then released to the plant cells (Jakobsen et al., 1992). The activated AM fungal phosphate transporters (PTs) absorb external inorganic phosphate (Pi) into the extraradical hyphae (Harrison and van Buuren, 1995, Maldonado-Mendoza et al., 2001 and Fiorilli et al., 2013) and Pi accumulates in the vacuoles of extraradical hyphae as polyphosphate (polyPi) (Ezawa et al., 2003). PolyPi chains are thought to be transferred by a tubular vacuolar network (Timonen et al., 2001 and Uetake et al., 2002) into the intraradical hyphae and arbuscules, where the Pi is hydrolyzed from polyPi by a fungal phosphatase and exopolyphosphatase, after which the Pi is released into the plant interfacial apoplast of arbuscules (Javot et al., 2007). To date, the mechanism by which phosphate is released from the fungus to the arbuscules is unknown.
Once the phosphate from the intraradical mycelia is released into the periarbuscular space (PAS), the plant imports it into root cells via the expressed mycorrhiza-specific PTs located in the periarbuscular membrane (PAM) (Harrison et al., 2002). These PTs expressing in arbuscule-containing cells have recently been functionally characterized in AM symbionts of potato, legumes, rice, and poplar (Rausch et al., 2001, Javot et al., 2007, Loth-Pereda et al., 2011 and Yang et al., 2012). Similarly, AM fungi essentially contain phosphate transporter genes; for example, GvPT, GiPT, and GmosPT genes have been isolated from the AM fungi Glomus versiforme, Rhizophagus irregularis, and Funneliformis mosseae, respectively (Harrison and van Buuren, 1995, Maldonado-Mendoza et al., 2001 and Benedetto et al., 2005). These fungal PT genes that have been identified so far are located in the extraradical hyphae, thus suggesting their roles in Pi acquisition from the soil. GmosPT and GintPT are also expressed in the intraradical fungal structures (Balestrini et al., 2007 and Fiorilli et al., 2013), thus

indicating that these transporters may play potential roles in intraradical hyphae and arbuscules. This finding raises new questions about the function of AM fungal PTs during AM symbiosis.

Mycorrhizal plants regulate carbon allocation depending on the phosphate homeostasis in the cells (Fitter, 2006 and Helber et al., 2011) regarding the reciprocal rewards that stabilize cooperation in plant–mycorrhizal mutualism (Kiers et al., 2011); in turn, their fungal symbionts enhance the cooperation by increasing phosphate transfer to the roots, supplying more carbohydrates. Although the fungal PTs are regulated in response to the ambient phosphate, current knowledge on the effect of carbon on the expression of AM fungal PT genes is still unclear.

Recent studies have revealed that some nutrient transporters also have a receptor function. Thus, the presence of the two properties in these transporters: a transporter and a receptor, identified them as nutrient transceptors. In yeast, the phosphate transceptor Pho84 is capable of transporting phosphate and triggering the protein kinase A (PKA) signaling cascade (Popova et al., 2010). In addition, the nitrate transporter NRT1.1 of Arabidopsis thaliana also functions as a nitrate transceptor that not only takes up nitrate from the environment but also mediates the nitrate signaling pathway (Ho et al., 2009 and Gojon et al., 2011). However, the signaling functions of AM fungal PTs studied so far remain unknown.

Answering these questions requires the molecular characterization of fungal transporters operating at the plant–fungus and fungus–soil interfaces. However, it is nearly impossible to knock out the AM fungal PTs to determine the roles of them in AM symbiosis due to the obligate biotrophic nature and the hugely complex genetics of AM fungi (Sanders, 1999). Host-induced gene silencing (HIGS), whereby a gene is silenced in the symbiont by expressing an RNA interference construct in the host, provides a potential tool to address gene function in obligate biotrophic pathogenic and AM fungi (Nowara et al., 2010 and Helber et al., 2011).

In such a context, to further advance our understanding of phosphate transport by AM fungi, we characterized the Pi-responsive GigmPT encoding a high-affinity phosphate transporter from Gigaspora margarita that is required for AM symbiosis. We showed that GigmPT functioned as a phosphate sensor in the regulation of phosphate signaling (PHO) and PKA pathways in G. margarita, and could mediate phosphate transport and signaling in yeast. We further identified the amino acid residues exposed in the phosphate-binding site of GigmPT and showed that the same site was used for both transport and signaling.

Results

Identification of GigmPT, which Encodes a Predicted Phosphate Transporter

A full-length GigmPT cDNA clone (KC887075) was isolated from the cDNAs of G. margarita supplied with low phosphate by using RT–PCR with degenerate primers based on other known PTs. GigmPT shares 56%, 17%, 18%, and 46% amino acid sequence identity with GiPT, GiPT2, GiPT4, and PHO84 PTs from R. irregularis (Tisserant et al., 2012 and Tisserant et al., 2013) and Saccharomyces cerevisiae, respectively (Supplemental Table 1). The PCR-based strategies (see Methods for details) were also employed to isolate the genomic sequence of GigmPT, which is 3476 bp in length and contains an open reading frame flanked by 1488 bp of promoter sequence at the 5′ end and an 84-bp-long untranslated region at the 3′ end (Supplemental Figure 1A). Southern blot assays indicated that a single copy of GigmPT is present in the G. margarita genome (Supplemental Figure 1B). In silico

analysis revealed that GigmPT encoded a putative membrane-integrated protein of 543 amino acids, and the deduced GigmPT protein comprised 12 transmembrane domains (TMDs) with an intracellular central loop between TMD VI and TMD VII, and a cytosolic N and C terminus (Supplemental Figure 2). BLAST searches of the transporter categories indicated that GigmPT is a member of the major facilitator superfamily (MFS). The predicted 3D model suggests that GigmPT is highly conserved when compared with PiPT from Piriformospora indica (Pedersen et al., 2013) (Figure 1A and 1B). Furthermore, the 3D homology model of GigmPT based on the glycerol-3-phosphate transporter (GlPT) of Escherichia coli as template (Huang et al., 2003 and Yadav et al., 2010) shows the hollow barrel structure of MFS (Figure 1C and 1D), indicating that the GigmPT protein structure is conserved across bacteria and fungi. An unrooted phylogenetic tree showed the close relationship between GigmPT and other AM fungal Pi transporters (Figure 1E).

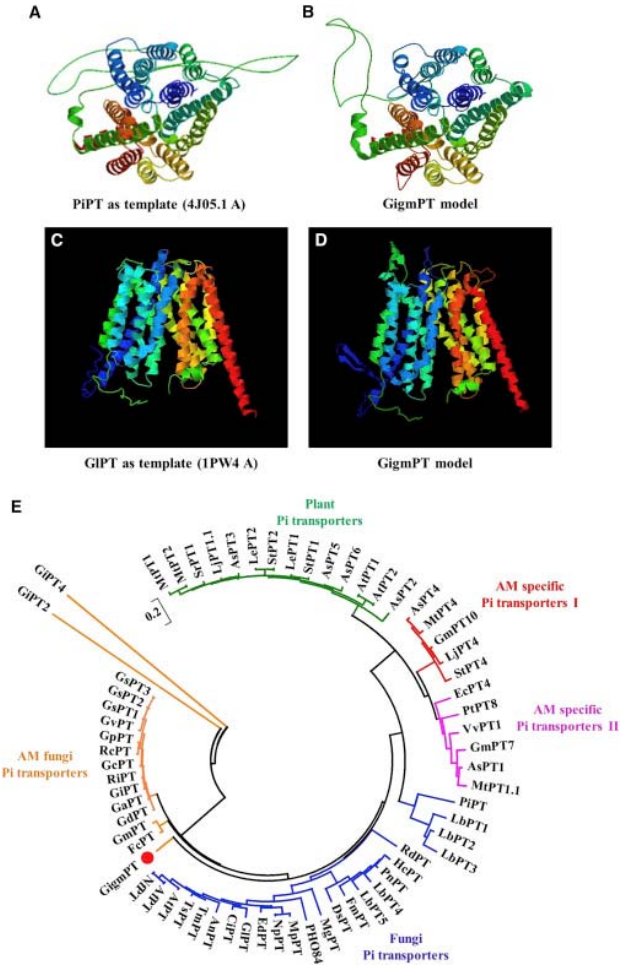

Figure 1. The Pi Transporter GigmPT in Gigaspora margarita.
(A–D) Conservation of protein 3D structures of GigmPT, PiPT, and GlPT. The 3D structures of GigmPT model (B and D) were assembled according to homology modeling by using PiPT from P. indica(A) and glycerol-3-phosphate transporter (GlPT) of E. coli(C) as templates, respectively. The PDB IDs of PiPT and GlPT are 4J05.1 and 1PW4, respectively; the chain is A.
(E) Phylogenetic tree of GigmPT (red circle) and other Pi transporters from fungi and plants. The unrooted phylogenetic tree was established based on neighbor-joining strategy using MEGAv4.1 software. Bootstrap tests were performed using 1000 replicates. Names and accession numbers of all the Pi transporters are provided in Supplemental Materials and Methods.

To search for putative cis-regulatory elements present in the promoter region of GigmPT, we isolated the 5′ flanking sequence of this gene using inverse PCR. The in silico analysis (see Supplemental Results) suggested that the PHO4-like DNA-binding consensus CACATG and the carbon-response elements CWTCC and CGGANNA are present in the promoter region of GigmPT (Supplemental Figure 3).

GigmPT Encodes a Plasma Membrane-Localized Transporter and Functions as a High-Affinity Phosphate Transporter

To determine whether GigmPT functions as a phosphate transporter and to assess its substrate affinity, we expressed GigmPT in the high-affinity phosphate transport-deficient S. cerevisiae strain MB192 (pho84 mutant). The results showed that the yeast cells expressing GigmPT gene were able to grow well under Pi deficiency, whereas the yeast mutant impaired cell growth (Figure 2A). Thus, the GigmPT transporter from G. margarita can complement the growth defect of the yeast pho84 mutant under low-Pi conditions. We further confirmed the subcellular localization of the GigmPT transporter and plasma membrane markers by fusing their C termini to eGFP. Consistent with its predicted hydropathy and function, the expression in yeast cells revealed that the GigmPT–eGFP fusion is targeted to the plasma membrane (Figure 2B). Fluorescence microscopy analysis of yeast cells expressing the plasma membrane (PM) marker PHO84 or GintAQPF1 further validated the PM localization of the PHO84 and GintAQPF1 transporters (Li et al., 2013), while the eGFP signal from GintAQPF2 was also detected at the periphery and cytoplasm of the yeast cells. In contrast, a high level of the eGFP signal was homogenously present inside the cytoplasmic control cell (Figure 2B). In addition, GigmPT protein colocalized to the plasma membrane in yeast cells along with PM marker PHO84 (Figure 2C). These data confirmed that GigmPT encodes a functional plasma membrane-localized transporter.

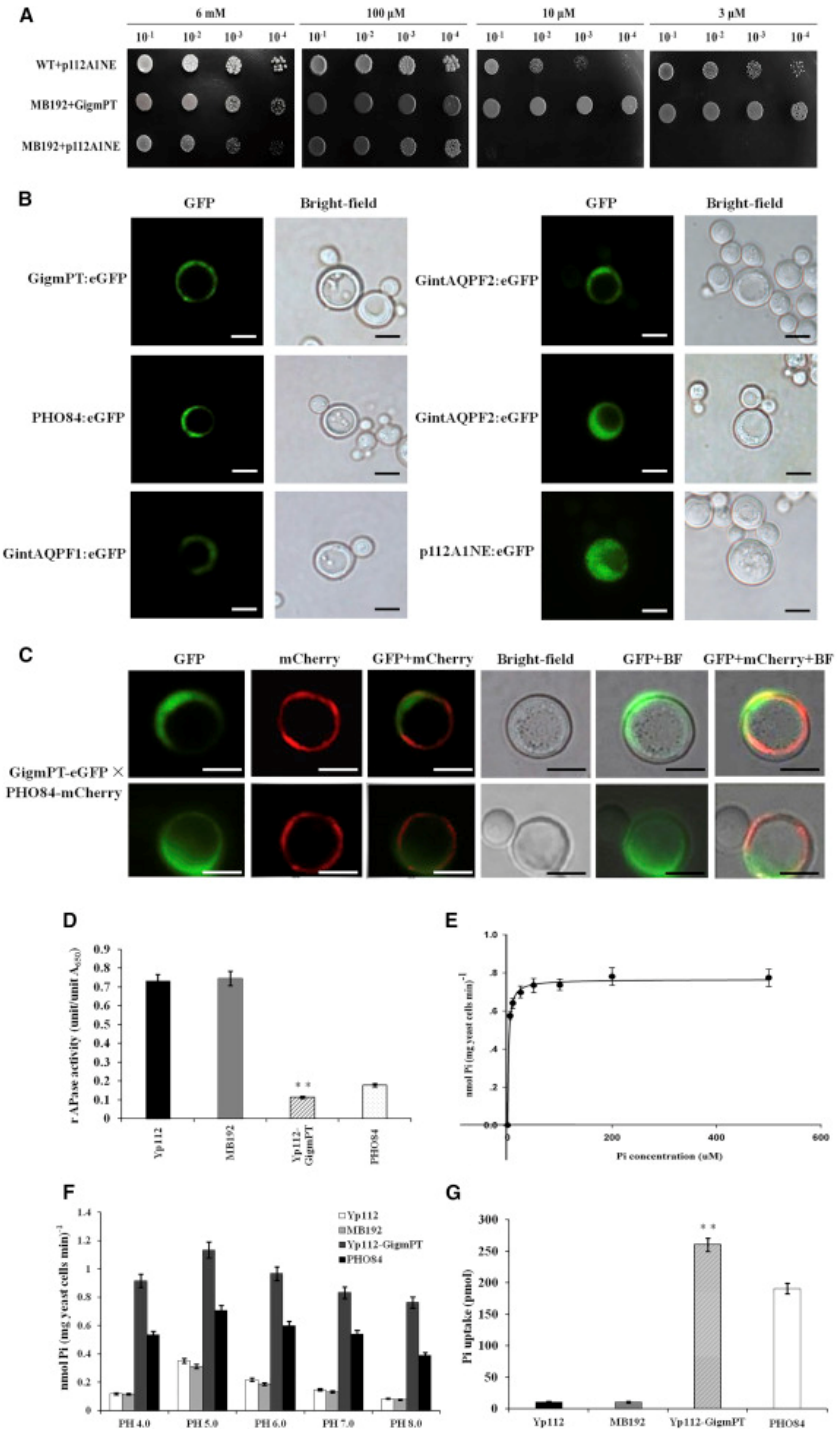

Figure 2. Functional Characterization of GigmPT Gene in Saccharomyces cerevisiae.
(A) The wild-type yeast cells harboring the empty vector (EV) p112A1NE (WT + p112A1NE), yeast MB192 carrying either the full-length cDNA of GigmPT (MB192 + GigmPT), or the EV (MB192 + EV) were grown in YNB medium. Equal volumes of 10-fold serial dilutions were plated on plates containing 6 mM Pi, 100 μM Pi, 10 μM Pi, or 3 μM Pi.
(B and C) Subcellular localization of GigmPT in yeast cells. (B) The GFP fluorescence images of each transporter-eGFP fusion are exhibited in the left panels, while the right panels indicate bright-field views. The PHO84 and GintAQPF1 proteins (Li et al., 2013) were presented as the plasma membrane markers, whereas GintAQPF2 showed an intracellular membrane marker (Li et al., 2013). The p112A1NE harboring eGFP (p112A1NE-eGFP) was the cytoplasmic control (pAdh:eGFP). (C)

Colocalization of GigmPT and PM marker PHO84 in yeast cells (upper and lower panels) by confocal microscopy. Localization of GigmPT-eGFP with PHO84-mCherry coexpression. Scale bars, 5 μm.
(D) Acid phosphatase activity was detected in transformed yeast MB192.
(E) Michaelis–Menten curve of 32Pi uptake at pH 5.0 under different Pi level. The time period was 15 min.
(F) Uptake of substrate 32Pi at different pH values.
(G) Pi uptake into yeast MB192 (gray), MB192 with EV (black), PHO84 (white), or GigmPT (gray plus line).
Yp112, MB192 carrying empty p112A1NE; GFP, green fluorescent protein; eGFP, enhanced GFP; WT, wild-type. Error bars represent SD values; n = 3. **P < 0.01.

We then tested the repressible acid phosphatase (rAPase) activity modulated by the GigmPT transporter in the Δpho84 mutant background (the MB192 strain, Bun-Ya et al., 1991), which can produce an rAPase. As expected, the MB192 or MB192 with empty vector (EV) strains exhibited high rAPase activity (Figure 2D), whereas in comparison the Δpho84 mutant strain expressing GigmPT or PHO84 showed very low rAPase activity. In agreement with the complementation observed in yeast cells (see Figure 2A), the data suggested that the expression of GigmPT or PHO84 restored cell growth.
To examine the Pi transport properties of GigmPT in the Δpho84 background, we measured the phosphate uptake kinetics in the MB192 strain expressing GigmPT. The uptake 32P of GigmPT transporter in MB192 followed Michaelis–Menten kinetics. The Km value was 1.8 ± 0.7 μM (Vmax 0.74 ± 0.08 nmol/min) (Figure 2E), suggesting that the GigmPT transporter can mediate high-affinity Pi acquisition. The pH optimum for GigmPT was 5.0 (Figure 2F). Similarly to the strain with PHO84, the MB192 strain expressing GigmPT acquires the amount of 32P much higher than the MB192 mutant (Figure 2G). These results demonstrate that GigmPT serves as a Pi/H+ symporter. These data combined with functional assays in yeast cells indicate that GigmPT functions as a high-affinity phosphate transporter.

GigmPT Is Expressed Both in the Intraradical and Extraradical Mycelium
To examine the symbiotic stage at which GigmPT is expressed, quantitative RT–PCR (qRT–PCR) was used to estimate the expression levels of GigmPT in G. margarita. As an additional marker for fungal gene expression in AM symbiosis, we detected the expression of GigmALP (Aono et al., 2004), which is constitutively expressed in mycorrhizal roots. The expression levels of GigmALP were higher in mycorrhizal roots than in other fungal tissues, while the results revealed that GigmPT was highly expressed both in mycorrhizal Astragalus sinicus roots and in extraradical mycelium (Figure 3A).

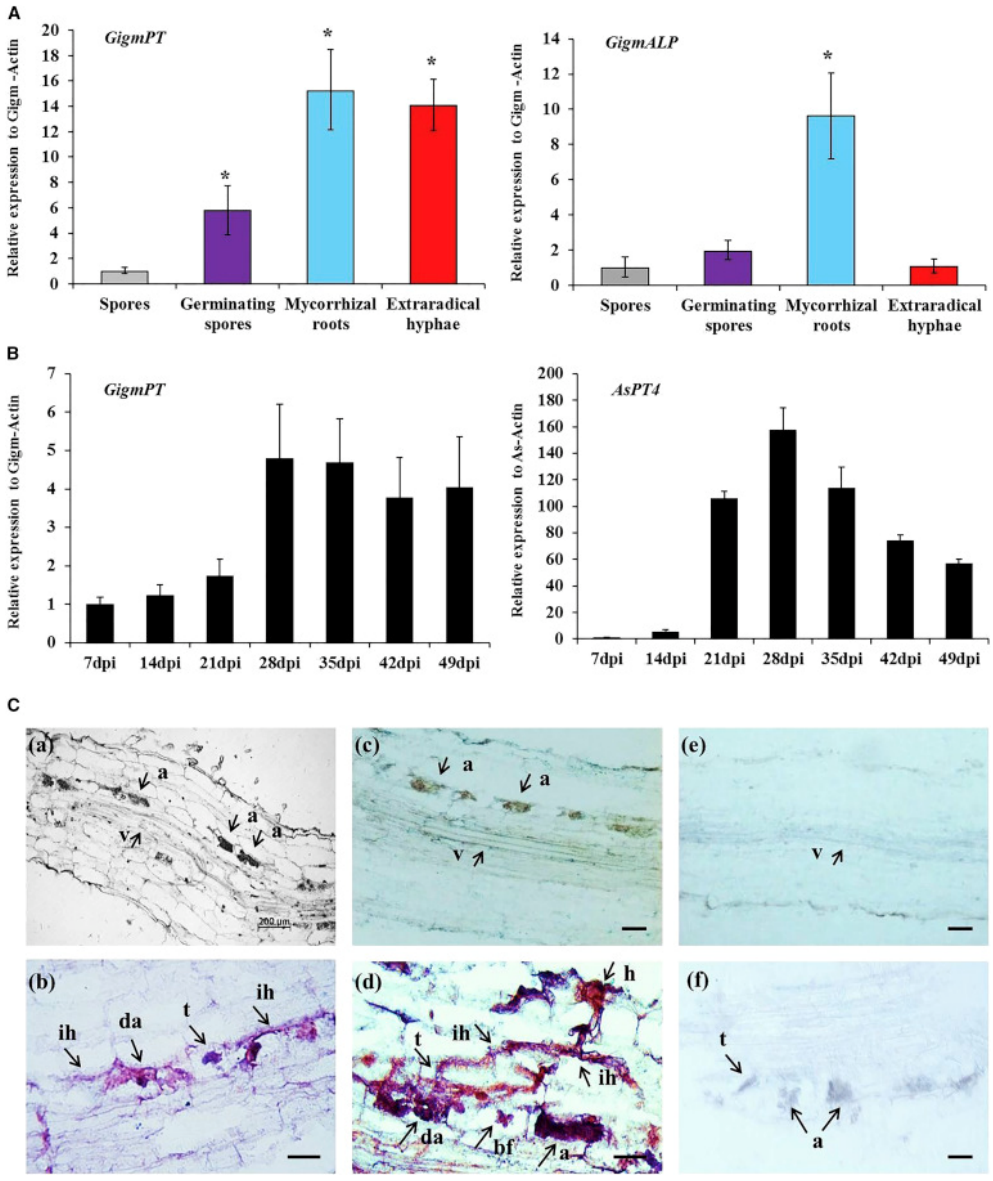

Figure 3. Expression Patterns of Phosphate Transporter GigmPT from the AM Fungus G. margarita.
(A) Expression levels of GigmPT and ALP in different fungal tissues: quiescent spores, germinating spores, mycorrhizal A. sinicus hairy roots, and extraradical hyphae. G. margarita alkaline phosphatase (ALP) was used as a marker gene; actin from G. margarita was used as the internal standard. Error bars represent the means of three biological replicates with SD values. *P < 0.05.
(B) Time-course assay of the expression of GigmPT and A. sinicus AsPT4 in mycorrhizal roots 7, 14, 21, 28, 35, 42, and 49 days post inoculation (dpi). GigmPT and AsPT4 genes are expressed as a ratio relative to Gigm-Actin and As-Actin transcripts, respectively. Error bars represent the means of three biological replicates with SD values.
(C)In situ hybridization of A. sinicus roots colonized with G. margarita. (a) Overview of a longitudinal section from mycorrhizal A. sinicus root. (b–d) Longitudinal sections from AM roots were probed with digoxigenin-labeled antisense RNA probe for GigmPT. (e) Section from nonmycorrhizal roots was probed with antisense probe as a blank control. (f) Section from AM roots was probed with a sense probe as a negative control. h, hyphopodia; t, arbuscule trunks; bf, bird's foot structure; da, developing arbuscules; a, mature arbuscules; ih, intraradical hyphae; v, vascular tissues. Scale bars represent 200 μm (a) and 50 μm (b–f).

To gain insight into the expression profiles of GigmPT gene during AM symbiosis, we performed qRT–PCR with A. sinicus roots colonized with G. margarita. The dynamics of arbuscule level in roots was confirmed by the expression of AM-specific Pi transporter gene AsPT4, which is particularly expressed in arbusculated cells and therefore an indicator of the function of AM symbiosis (Xie et al., 2013). It was found that the expression profiles of GigmPT were similar to that of AsPT4 over time (Figure 3B). Interestingly, a stable and high expression level of GigmPT was also observed during the later stages of AM symbiosis (Figure 3B), indicating that GigmPT was transcriptionally activated at other fungal structures besides arbuscules. To determine the specific localization of GigmPT expression in the intraradical structures of the fungus, we performed in situ hybridization analysis in the A. sinicus roots colonized with G. margarita (Figure 3Ca). Positive purple signals indicated the expression of GigmPT at intraradical hyphae and arbuscule trunks (Figure 3Cb and 3Cd). Importantly, the expression of GigmPT was also detected in birdsfoot, representing a stage characterized by low-order branching organized in a bird's foot-like structure (Gutjahr and Parniske, 2013), and arbuscules (Figure 3Cc and 3Cd), suggesting that these structures are possible sites of phosphate reuptake. As expected, the transcript accumulation of GigmPT was not present in nonmycorrhizal and negative control roots (Figure 3Ce and 3Cf). Taken together, these results from the expression profiles and localization of GigmPT gene in mycorrhizal roots imply that the GigmPT transporter might be able to reabsorb phosphate from the peripheral apoplast and the PAS at the intraradical hyphae and arbuscules, respectively.

GigmPT Protein Is Present in Arbuscules and Intraradical Hyphae

To further determine whether the GigmPT protein is present in the arbuscules and intraradical hyphae, we harvested AM roots grown in cultures with low-phosphate (3 μM Pi) or high-phosphate (300 μM Pi) supply and immunostained them with the GigmPT-specific antibody. The immunostaining signals of GigmPT were detected in mycorrhizal roots through the green or red fluorescence of a secondary antibody conjugated to Alexa Fluor 488 or Alexa Fluor 568, respectively, while the mycorrhizal roots were counterstained with the WGA–Texas red conjugate to visualize the fungus. The cells with arbuscules showed strong red fluorescent signals arising from the WGA–Texas red conjugate, and the corresponding images exhibited green fluorescence (Figure 4A–4D and Supplemental Figure 5A), suggesting the presence of GigmPT colocalized to the same fungal cells. Figure 4 shows the images of several arbuscules and the intraradical hyphae. The highly dichotomous branches of arbuscules were visible, and the immunostaining signals of GigmPT colocalized with the arbuscules (Figure 4A and 4B). In contrast, negative control with GigmPT pre-immune serum did not immunostain the arbuscules (Supplemental Figure 5B).

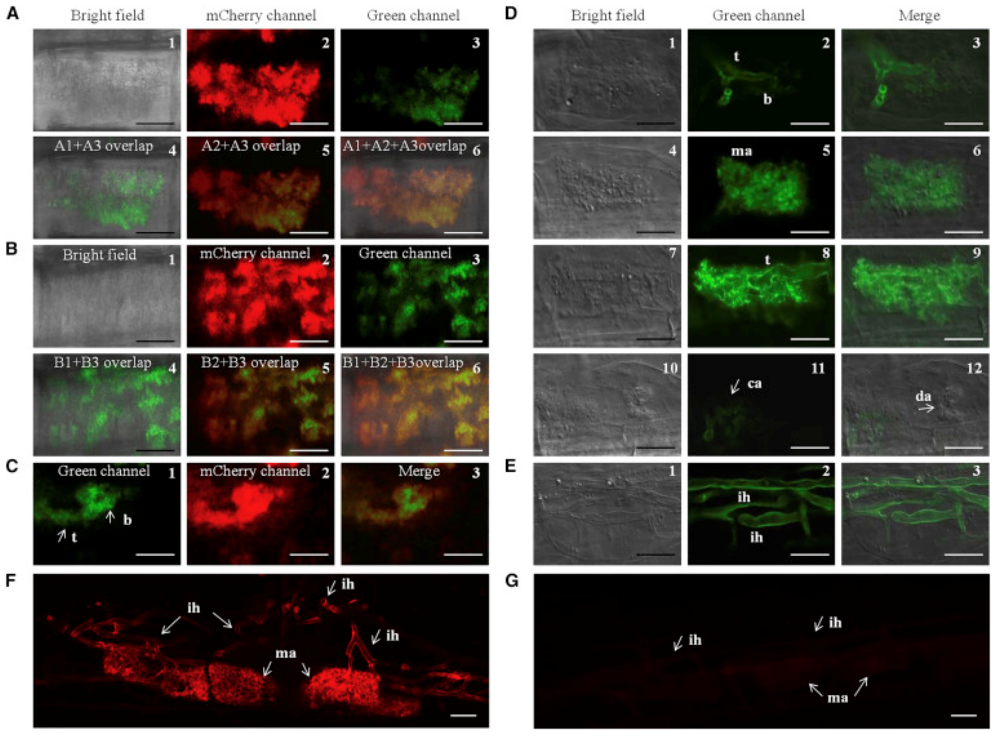

Figure 4. Immunolocalization of GigmPT.
(A–C) Epifluorescence microscopy images of AM roots (A3, B3, and C1) probed with GigmPT antibodies visualized with a secondary antibody conjugated with Alexa Fluor 488. Corresponding images in bright field (A1 and B1). Corresponding images (A2, B2, and C2) showing red fluorescence from WGA–Texas red staining. Merged images showing both bright-field and green fluorescence (A4, B4), or both red and green fluorescence (A5, B5, and C3). Overlaps of bright-field, red fluorescence, and green fluorescence images are shown (A6 and B6). Mycorrhizal plants grown in pots in the presence of either 300 μM (A) or 3 μM (B and C) phosphate.
(D–G) Confocal microscopy images of AM roots probed with GigmPT antibodies. Nomarski views of an arbuscule trunk (D1), a mature arbuscule (D4), a degenerating arbuscule (D7), a collapsed arbuscule (D10), and intraradical hyphae (E1) are shown. (D2, D5, D8, D10, and E2) Corresponding images showing green fluorescence from GigmPT immunostaining. (D3, D6, D8, D12, and E3) Merged images showing both bright-field and green fluorescence. (F) Antibodies to GigmPT were detected with a secondary antibody conjugated with Alexa Fluor 568. (G) Immunostaining with GigmPT pre-immune serum to test the specificity of the antibody. t, arbuscule trunks; b, branches of the arbuscules; ma, mature arbuscule; ca, collapsed arbuscule; da, dead arbuscule; ih, intraradical hyphae.
Scale bars represent 50 μm. Detailed descriptions of the images are provided in the Supplemental data.

Figure 4A showed weak fluorescent signals in the mature arbuscule in the presence of Pi, whereas the immunostaining signals of GigmPT protein were abundantly observed in arbuscule under Pi-starvation conditions (Figure 4B). This result was confirmed on the protein level with the former observation of Pi-starvation-dependent accumulation of GigmPT transcripts in AM roots (Supplemental Figure 4). Therefore, immunolocalization by GigmPT antibody was more abundantly found in arbuscules under Pi deficiency.
Figure 4C and 4D show images of roots containing arbuscules at early, developing, and collapsed stages, and a GigmPT signal was clearly visible in the very young arbuscule, which displayed only the first dichotomous branch (Figure 4C.1), while the immunostaining signal was also found in the arbuscule trunk (Figure 4D.2). Indeed, the developing arbuscule showed a strong immunostaining signal (Figure 4D.5) when compared with the completely collapsed arbuscule (Figure 4D.11), and the GigmPT

signal was also obviously detected in the degenerating arbuscule (Figure 4D.8). These results indicated that the expression of GigmPT protein is coordinated with the lifespan extension of arbuscules.
In addition, the green signal was also apparently detected within intraradical hyphae beside the arbuscules (Figure 4E). The GigmPT antibody was also determined with the secondary antibody conjugated to Alexa Fluor 568, and the red signal captured by confocal microscope of the immunostained intraradical structures represented the PM localization of GigmPT in the arbuscules and intraradical hyphae (Figure 4F). Negative control using the GigmPT pre-immune serum did not display the specific immunostaining signal (Figure 4G).
Taken together, immunostaining of GigmPT reveals that GigmPT protein is present in the arbuscules, arbuscule trunks, and intraradical hyphae within the roots as expected from the previously observed transcript localization (Figure 3C), and is located in the PM of arbuscules and intraradical hyphae.

GigmPT Expression Depends on Phosphate Availability
We next asked whether the expression of GigmPT would be responsive to ambient phosphate availability during AM symbiosis. qRT–PCR was performed to estimate GigmPT expression in mycorrhizal roots and extraradical mycelium (ERM) subjected to different Pi concentrations. GigmPT is expressed in mycorrhizal roots and ERM in response to micromolar levels of phosphate. We detected increased expression of GigmPT at 65 μM Pi or less, compared with the mycorrhizal roots exposed to higher Pi (300 μM) (Supplemental Figure 4A and 4B), and the ERM of G. margarita exposed to the low Pi concentration also showed an increase in transcription level of GigmPT (Supplemental Figure 4C and 4D). The upregulated expression of GigmPT in both mycorrhizal roots and ERM under Pi deficiency is consistent with the previous observation that GigmPT is a high-affinity transporter.
For further determination of whether the Pi was directly acquired by the ERM, the ERM was grown in liquid medium in the presence of 3, 30, or 300 μM Pi and then exposed for 14 days to the medium. We next quantified the free Pi concentrations, polyphosphate, and alkaline phosphatase (ALP) activity in ERM exposed to either a low- or high-Pi regime. The results showed that the Pi concentrations of ERM exposed to high Pi were significantly increased, whereas the residual Pi concentrations of liquid medium were lower than that of initial Pi application (Supplemental Figure 4E), in addition, the ERM exposed to high Pi accumulated much more polyphosphate and increased the levels of ALP activity (Supplemental Figure 4F). These findings suggested that the ERM was indeed able to take up phosphate from medium.

GigmPT Expression Is Rapidly Induced by Carbon in Pi-Deprived Mycelia
To test the hypothesis that the exchange of P and C are interconnected (Helber et al., 2011), we added amounts of sucrose ranging from 3 mM to 90 mM to mycorrhizal hairy roots growing in different Pi media. Since it cannot be directly taken up by AM fungus, the sucrose must be first utilized by the mycorrhizal roots and then supplied to the fungus in the form of hexoses. Pi contents in mycorrhizal roots occur in response to sucrose availability, and vice versa. The repleted Pi in the fungal compartment has an effect on the allocation of sucrose to extraradical mycelia (Supplemental Figure 6A and 6B).
The previous in silico analysis of the promoter of GigmPT indicated that this gene might respond to carbon. To investigate whether expression levels of G. margarita

PTs were affected by sucrose availability, we analyzed the transcription levels of GigmPT, GigmPT1, and GigmPT2 genes in the ERM and IRM of G. margarita grown in bi-compartments in the presence of either 0, 3, 30, or 90 mM sucrose and exposed for 14 days to a low-Pi (3 μM) or high-Pi (300 μM) medium. The transcript levels of GigmPT in ERM but not IRM increased with the availability of sucrose when fungus was grown in low-Pi medium. Nevertheless, in the presence of Pi, GigmPT expression in ERM or IRM was not affected by the sucrose supply (Supplemental Figure 7A). Under low-Pi conditions, the expression pattern of GigmPT1 was similar to that of GigmPT gene in both mycelia, but there was opposite regulation of GigmPT1 in ERM and IRM at abundant Pi levels (Supplemental Figure 7B). In contrast with the expression profiles of GigmPT and GigmPT1 genes previously observed, transcription of GigmPT2 in both mycelia was apparently downregulated in response to increased sucrose levels, irrespective of the ambient Pi availability (Supplemental Figure 7C). In addition, transcript levels of AM-specific AsPT1 and AsPT4 genes were upregulated in mycorrhized roots that had been supplemented with sucrose, regardless of the Pi levels (Supplemental Figure 7D).

To further determine the effect of sucrose on GigmPT gene by time-course analysis, we analyzed GigmPT expression in both mycelia of G. margarita grown in either low- or high-Pi medium after the addition of 30 mM sucrose to the root compartment. GigmPT gene expression was performed 1, 2, 7, and 14 days after sucrose treatment. Under Pi-starvation conditions, transcription of GigmPT was rapidly induced in both mycelia in the presence of sucrose (Supplemental Figure 7E), while the addition of sucrose to the Pi-repleted mycelia had no effect on GigmPT transcription at all the time points analyzed (Supplemental Figure 7F). Importantly, these concurrent changes in the plant and fungal PT gene expression were also accompanied by an increase in Pi transport (Supplemental Figure 6C and 6D). We observed no phenotypic differences in both the mycorrhizal colonization (Supplemental Figure 8A and 8B) and the absolute content of fungal tissues within the mycorrhizal roots subjected to various sucrose concentrations (Supplemental Figure 8C and 8D). Taken together, our data revealed that the expression of GigmPT is connected to the symbiotic carbon supply under Pi deficiency, and three AM fungal PT genes were differentially expressed in intra- and extraradical fungal structures and in response to carbon.

GigmPT Is Required for AM Symbiosis

A gene knockdown experiment was performed to examine the importance of GigmPT to AM symbiosis by using a HIGS strategy (Nowara et al., 2010 and Helber et al., 2011). The RNAi-silencing vector was constructed using a 305-bp region at the 5′ end of GigmPT, as this region was very divergent from the sequences of PT genes both in G. margarita and A. sinicus. In the transformed roots, the transcript accumulation of the hairpin structure and double-stranded RNA of GigmPT was confirmed by RT–PCR and Northern blot analysis, and the small interfering RNAs (siRNAs) were also detected in GigmPT RNAi roots (Supplemental Figures 9 and 10). These results indicate that the transformed roots harboring GigmPT RNAi-silencing constructs constitutively expressed the specific siRNAs produced by the GigmPT gene, a prerequisite to explore the in vivo roles of GigmPT during AM symbiosis.

To determine whether silencing of GigmPT would affect the mycorrhization, we investigated the RNAi and control (EV) roots colonized with G. margarita to analyze the colonization 4 weeks after inoculation. The control roots exhibited much higher intensity of mycorrhiza and showed much more arbuscules than GigmPT RNAi roots,

particularly in RNAi-1 and -2 roots (Figure 5A and 5B). Observation of the arbuscule structure revealed that the arbuscule development in RNAi roots was defective: the majority of arbuscules were degenerating or dead and collapsed arbuscules contained septa, whereas arbuscules in control roots were mature with full branches (Figure 5A). Furthermore, the observed arbuscule classes showed the opposite size distribution in the EV and RNAi-2 roots (Figure 5C). In addition, we found a significant shift of mature arbuscules toward degenerating and collapsed or dead arbuscules in the RNAi-2 roots (Figure 5D), indicating that the arbuscule development switched to the senescence stage. A detailed description is provided in Supplemental Results.

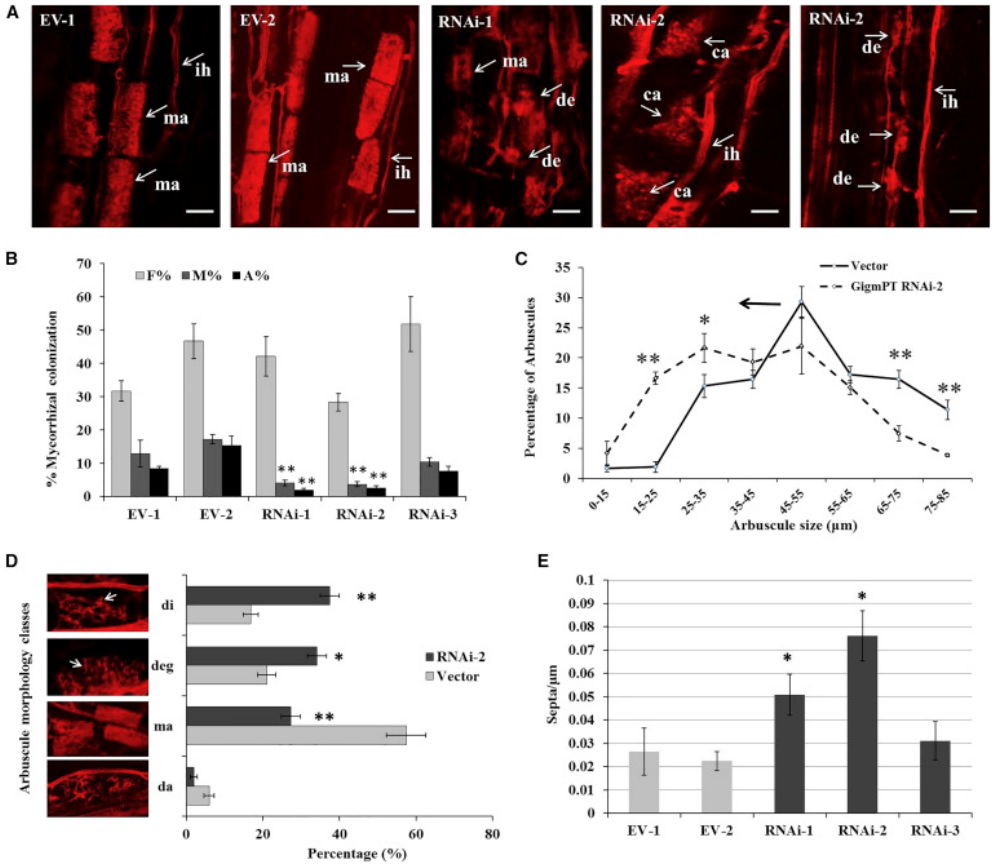

Figure 5. Arbuscular Mycorrhizal Phenotypes of Host-Induced Gene Silencing of GigmPT in Hairy Roots.

(A) Laser-scanning confocal microscopy images of G. margarita arbuscules in control (EV) and RNAi roots. Roots were stained with acid fuchsin. ih, intraradical hyphae; ma, mature arbuscules; ca, collapsed arbuscules; de, dead arbuscules. Scale bars represent 20 µm.

(B) Mycorrhization level was analyzed after acid fuchsin staining of GigmPT RNAi hairy roots in comparison with control roots (EV) 28 dpi with G. margarita. F%, frequency of colonization; M%, intensity of mycorrhiza; A%, arbuscule abundance. Error bars represent ± SD; n = 5, five technical replicates.

(C) Analysis of arbuscule development in RNAi-2 line inoculated with G. margarita. Vector, EV-1. Data are from the means of at least 10 arbuscules and error bars represent SD of the means (n = 10).

(D) The population of arbuscule developmental stages in RNAi-2 and control roots. Vector, EV-1; da, ma, deg, and di represent developing arbuscules, mature arbuscules, arbuscules degenerating, and dead arbuscules, respectively. White arrows indicate septa. Values are the percentage of at least 10 arbuscules (n = 10) ± SD.

(E) Number of septa present in intraradical hyphae. Values are means ± SD of 20 infection units (n = 3). Asterisks indicate a statistically significant difference from respective vector control roots (*P < 0.05; **P < 0.01).

Intraradical hyphae can also serve as a potential site for nutrient exchange between host and symbiont (Parniske, 2008), while the septa in hyphae separate the senescent or dead fungal branches from the normal ones (Cox et al., 1980), indicating that the formation of septa impairs the development of AM fungi in roots. To test whether GigmPT function is essential for the hyphal growth of AM fungus within roots, we examined the effect of GigmPT RNAi lines on intraradical hyphae. The results show that downregulation of GigmPT has no effect on intraradical hyphae thriving inside the roots (see Supplemental Results and Supplemental Figure 11). However, relative to the controls, intercellular hyphae containing more septa were observed in RNAi-1 and -2 roots (Figure 5E).

Moreover, in composite plants knockdown of GigmPT also caused a dramatically reduced arbuscule development (Figure 6A–6I) and, similar to the phenotypes observed in RNAi-1 and -2 roots, the arbuscule morphology was abnormal: arbuscules were smaller with fewer branches and contained septa in comparison with control arbuscules (Figure 6 and see Supplemental Results). The observed phenotypes indicated that silence of GigmPT hampered the development of G. margarita inside the roots.

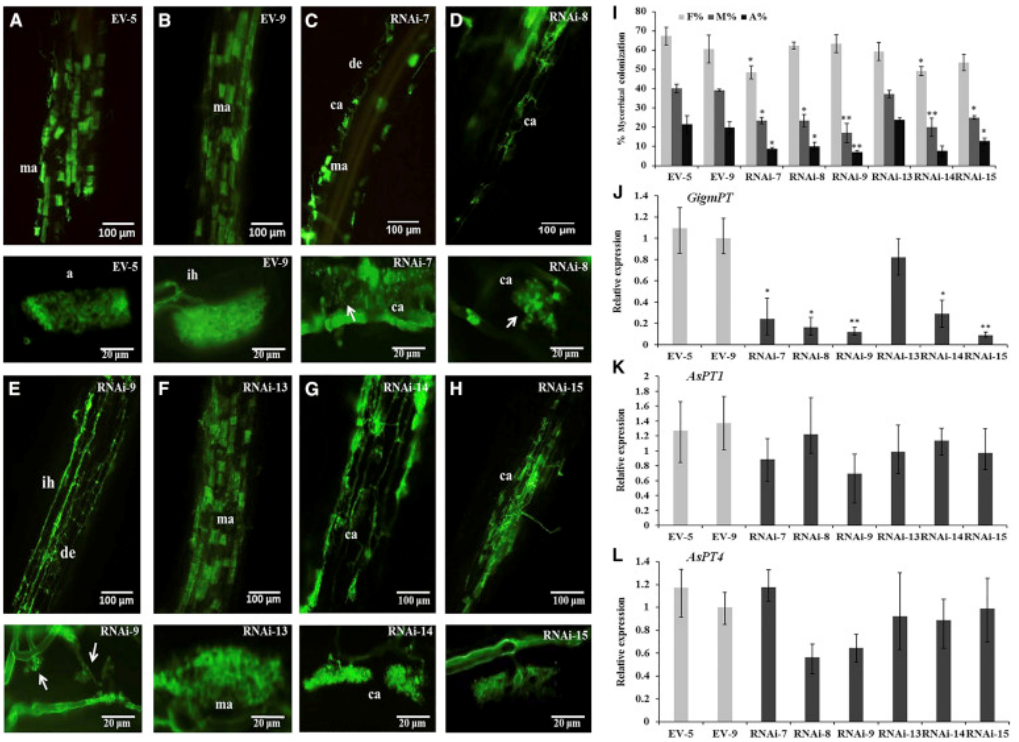

Figure 6. Mycorrhizal and Molecular Phenotypes of HIGS of GigmPT in Composite Plants.

(A–H)G. margarita arbuscule phenotype in HIGS of GigmPT. Fluorescence microscopy images of G. margarita infection units (top panels) and arbuscule morphology (bottom panels) in control (EV-5 and EV-9) and RNAi (RNAi-7, -8, -9, -13, -14, and -15) lines at 28 dpi. Roots were stained with WGA–Alexa Fluor 488 conjugate. Arrows indicate collapsed arbuscules with septa. ma, mature arbuscules; ca, collapsed arbuscules; de, dead arbuscules; ih, intraradical hyphae. Scale bar calibrations are indicated.

(I) Mycorrhization level was analyzed after WGA 488 staining of GigmPT RNAi roots in comparison with control roots (EV) 28 dpi with G. margarita. F%, frequency of colonization; M%, intensity of mycorrhiza; A%, arbuscule abundance.

(J–L) Expression levels of GigmPT, AsPT1 and AsPT4 in control (EV) and RNAi lines were determined by real-time RT–PCR. The actin gene was used as the reference gene.

The SD values were indicated. Asterisks indicate a statistically significant difference from respective vector control lines (*P < 0.05, **P < 0.01; n > 8, three technical replicates).

To detect the activity of the GigmPT gene in HIGS mutants, we examined expression levels of the fungal GigmPT, GigmPT1, and the AM-specific PT genes AsPT1 and AsPT4 (Xie et al., 2013) by qRT–PCR in mycorrhizal roots. Transcription of GigmPT was significantly reduced in the positive RNAi roots (Figure 6J and Supplemental Figure 9D). By contrast, the expression levels of GigmPT1, AsPT1, and AsPT4 were derepressed in comparison with the control roots (Figure 6K and 6L; Supplemental Figure 9D). The evidence of the absence of nontarget GigmPT1 and PT1/4 gene silencing thereby demonstrated that no off-target silencing was found for GigmPT RNAi triggers. Moreover, GigmPT was specifically downregulated in extraradical hyphae of G. margarita concerning the transcription of genes and the existence of siRNAs (Supplemental Figure 12 and see Supplemental Results). Taken together, these findings suggested that GigmPT is required for functional AM symbiosis, particularly for the development of functional arbuscules and intercellular hyphae, while a downregulation of GigmPT by HIGS impairs the development of symbiosis.

Repression of GigmPT Gene Affects PHO Signaling and PKA Targets in G. margarita

Homology searches in the first draft of the transcriptome of the G. margarita BEG34 (Salvioli et al., 2016) permitted us to characterize the expression profiles of the potential genes in G. margarita regarding the phosphate sensing and signaling networks (Supplemental Figure 13). We have identified orthologous proteins for each component of PHO and PKA pathways using TBLASTN searches and the R. irregularis transcriptome (Tisserant et al., 2012) to determine the conservation of PHO, PKA, and other related pathways in G. margarita. Utilizing a pre-determined cutoff e value of <1e-5, a majority of the components of the PHO and PKA pathways in R. irregularis have orthologs in G. margarita (Table 1), indicating that similar PHO and PKA pathways are present in G. margarita. G. margarita transcripts a new isoform of ALP2 absent in the R. irregularis transcriptome, at least two novel isoforms of SPX domain-containing proteins Syg1.1 and Syg1.2, or three additional isoforms of Pi transporters GigmPT2–4 (Table 1); however, G. margarita does not express the high-affinity Pi transporter Pho89 present in R. irregularis (Tisserant et al., 2012) or the regulatory factor SPL2 (Wykoff et al., 2007). In addition, the mitogen-activated protein kinase (MAPK) and target of rapamycin (TOR) signaling pathways also exist in G. margarita (Table 1 and Supplemental Figure 13).

Table 1 describes 63 unique genes possibly involved in phosphate sensing and signaling networks, all of them being distributed into four pathways with distinct genes. These genes were functionally annotated according to Gene Ontology and G. margarita Transcriptome Database (Salvioli et al., 2016). To create an expression profile of the effect of phosphate on the transcriptional changes of selected genes in G. margarita, we employed qRT–PCR analysis to evaluate the transcript levels of phosphate signaling-related genes or isoforms identified in the RNA-sequencing (RNA-seq) experiment (Salvioli et al., 2016; Supplemental Figure 13). A list of differentially expressed genes related to PHO, PKA, MAPK, and TOR signaling are shown in Table 1 and Figure 7. Some of these genes, such as those representing putative PTs (GigmPT1–5) and low-affinity transporters Pho87/90/91 (Hürlimann et al., 2007 and Hürlimann et al., 2009), PHO signaling, polyPi metabolism, reserve carbohydrate metabolism, and stress tolerance, were upregulated in G. margarita

during symbiosis grown in low Pi versus high Pi. However, those genes representing phosphate homeostasis, ribosome structure, growth regulation, and reproduction dropped less or exhibited an opposite expression profile.

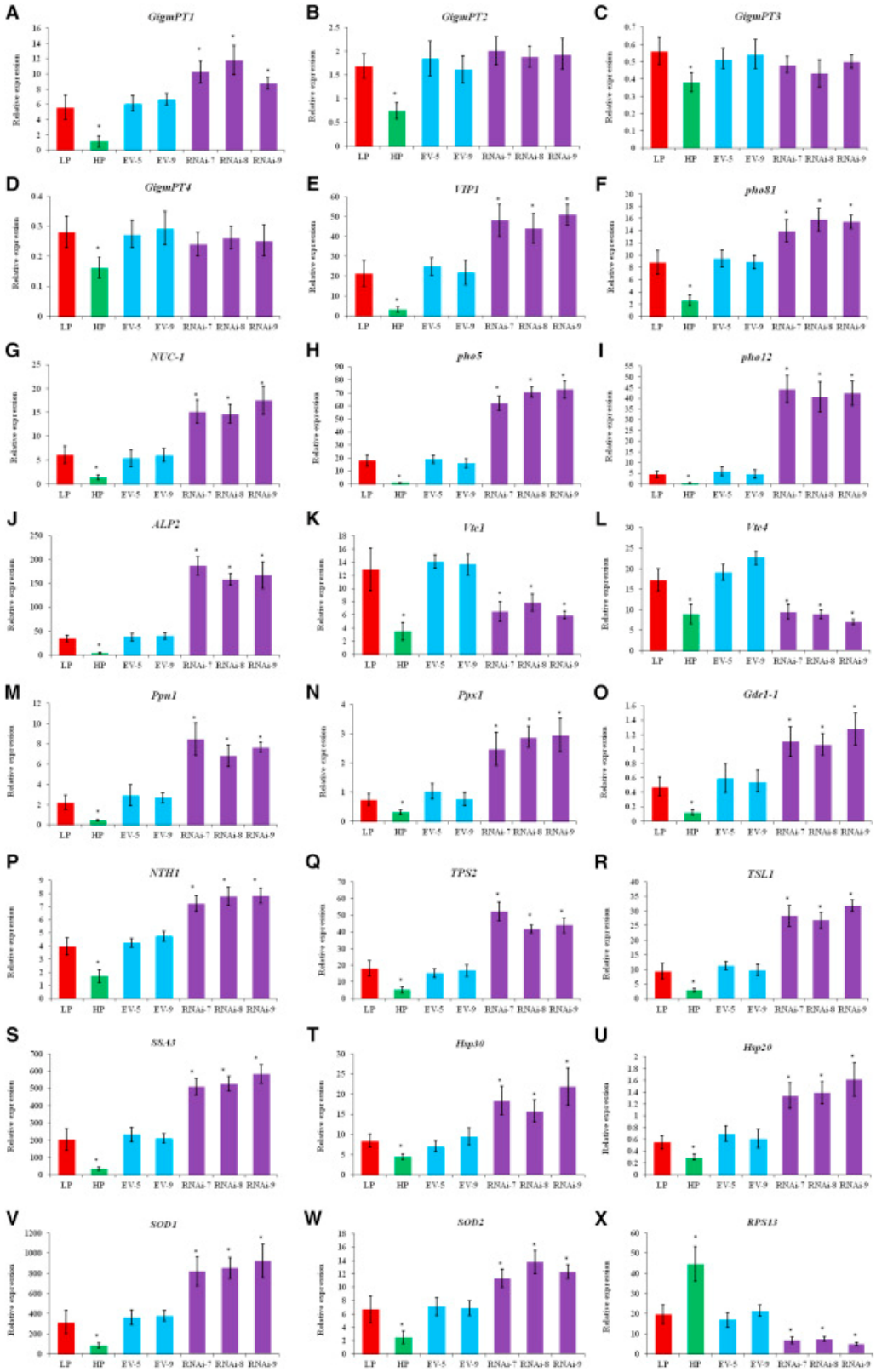

Figure 7. Loss Function of GigmPT Affects PHO and PKA Signaling Cascades.
The differentially expressed genes potentially involved in phosphate-responsive (PHO) and protein kinase A (PKA) signaling cascades, estimated by real-time qRT–PCR (A–X). The selected genes possibly regulated in response to phosphate or GigmPT RNAi mutants were amplified from the first-strand cDNA obtained from mycorrhizal roots inoculated with G. margarita grown in low-Pi (LP: 3 μM) or high-Pi (HP: 1 mM) medium, and from mycorrhizal roots of controls (EV-5 and EV-9) and GigmPT RNAi lines (RNAi-7, -8, and -9). The genes and corresponding accession numbers employed are listed in Table 1. The data represent mean values ± SD obtained from experiments. Statistically significant levels evaluated for LP and HP, or EV and RNAi lines are denoted by asterisks: *P < 0.05, Tukey's test.

To further investigate whether knockdown of GigmPT by HIGS analysis affects phosphate sensing- and signaling-related gene expression of G. margarita during symbiosis, we performed expression analysis of the selected genes in the control and RNAi lines through qRT–PCR (Table 1 and Figure 7). The transcript levels of PHO signaling genes, especially VIP1, Pho81, Pho2, NUC-1, GigmPT1, and GigmPT2, and genes involved in phosphate metabolism, such as Pho5, Pho12, ACP5, and ALP-2 for phosphate acquisition, PTs Pho87/90/91 for Pi homeostasis (Hürlimann et al., 2007 and Hürlimann et al., 2009), Gde1-1 and Gde1-2 for phosphate scavenging, and Ppn1 and Ppx1 for polyPi hydrolysis, were derepressed in RNAi lines compared with the respective control lines (Table 1 and Figure 7A–7O). We also showed that downregulation of GigmPT affects well-known PKA targets: induction of STRE-controlled genes (SSA3, Hsp30, Hsp20, SOD1, and SOD2) and genes involved in trehalose metabolism (NTH1, TPS2, and TSL1), but repression of genes encoding ribosome protein RPS13 (Table 1 and Figure 7P–7X).

Phosphate and Gly3P Can Activate PKA Signaling through the GigmPT Transceptor
Since GigmPT possesses phosphate transport capacity under Pi-limited conditions, and also is essential for the activity of G. margarita in the host, we hypothesized that GigmPT as a phosphate sensor may participate in the phosphate sensing and signaling pathways according to the above data (Figure 7). GigmPT also shows sequence and structural similarities to the yeast Pho84 sensor (Giots et al., 2003 and Popova et al., 2010). Based on these similarities, we further determined whether GigmPT could act as both a transporter and a receptor, or a “transceptor,” in yeast. We used the GigmPT-expressing yeast to test whether phosphate could trigger PKA signaling through GigmPT. The supplementation of Pi or organic phosphate esters to phosphate-starved cells triggered the PKA signaling pathway with regard to activating the PKA target (Supplemental Table 2). We also examined whether phosphate-containing compounds that typically are not transported by GigmPT can trigger phosphate signaling. Therefore, the compounds glycerol-3-phosphate (Gly3P) and phosphonoacetic acid (PAA) were selected as the ligands. The results showed that the addition of 10 mM Gly3P to the phosphate-starved yeast expressing GigmPT rapidly triggered PKA signaling comparable with that by phosphate addition (Figure 8A and Supplemental Table 2). In contrast, the organic phosphate ester PAA did not produce any significant activation of PKA signaling (Figure 8B). In the positive controls, the Pi sensor PHO84 and R. irregularis Pi transporter GiPT2 (Tisserant et al., 2012), which are functional in Pi transport-defective strains (data not shown), also activated PKA signaling in a similar manner, whereas the putative Na+/Pi symporter GiPT4 (Tisserant et al., 2012) served as a negative control regarding the existence of transport activity (data not shown) without signaling function (Figure 8A and 8B). Overall, GigmPT functions as a transceptor in response to phosphate. Furthermore,

Gly3P and PAA are competitive inhibitors of phosphate transport through GigmPT (see Supplemental Results).

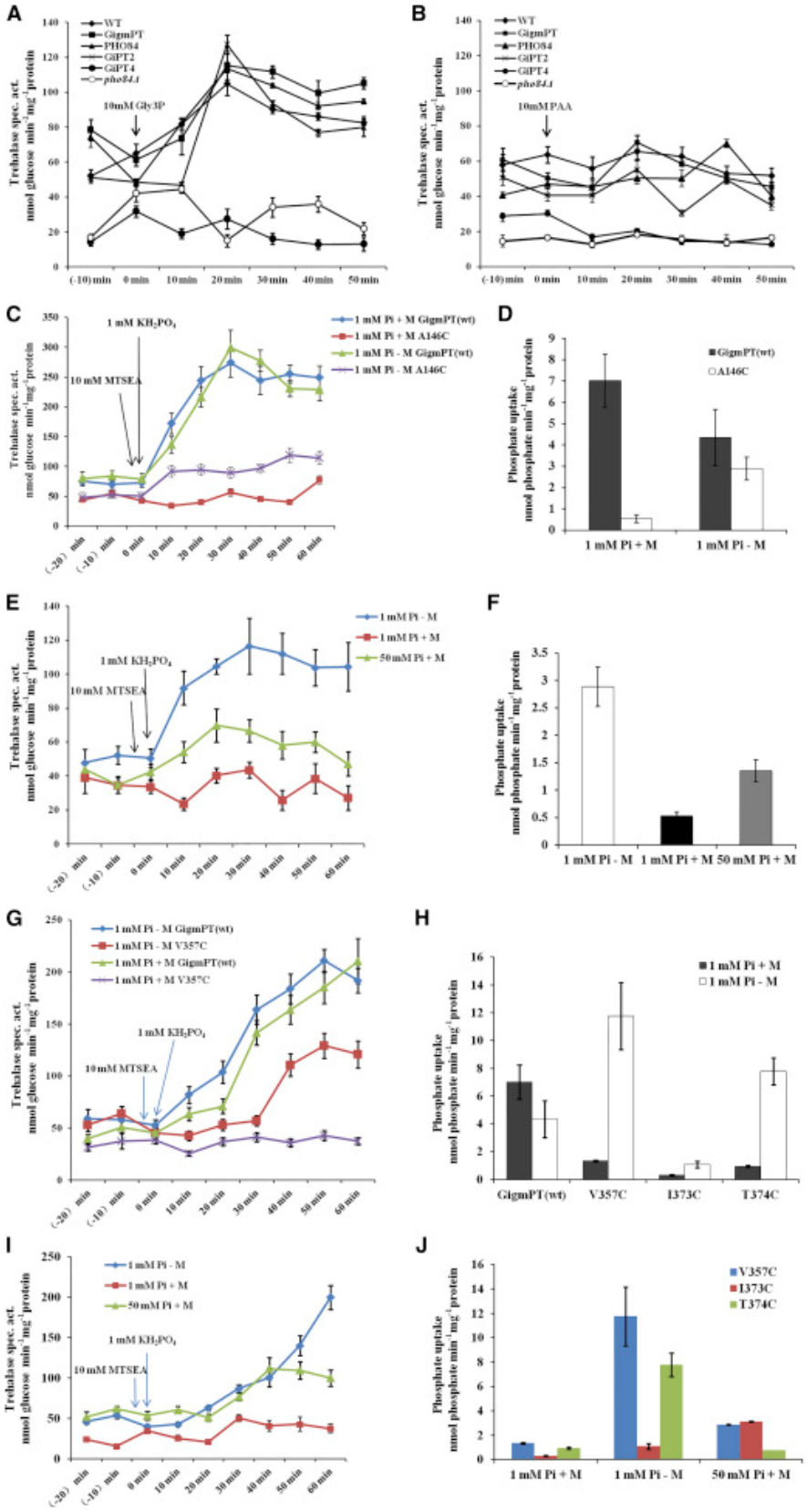

Figure 8. Transport and Signaling through the Phosphate-Binding Site of G. margarita GigmPT Phosphate Transceptor in Yeast.
(A and B) The increase in trehalase activity after addition of the 10 mM Gly3P (A) or phosphonoacetic acid (PAA) (B) compounds to phosphate-starved cells. Strains: wild-type (WT), pho84Δ:pGigmPT (GigmPT), pho84Δ:pPHO84 (PHO84), pho84Δ:pGiPT2 (GiPT2), pho84Δ:pGiPT4 (GiPT4), and pho84Δ. PHO84 and GiPT2 were employed as the positive controls, and GiPT4 as the negative control.
(C–J) SCAM analysis indicates that Ala146 in TMD IV (C–F) and Val357 in TMD VIII (G–J) are required for the phosphate-binding site of GigmPT. (C and G) Increase in trehalase activity after addition of 1 mM KH2PO4 to phosphate-starved cells of the pho84Δ:pGigmPT (WT) strain and the Ala146C(C) or Val357C(G) mutants without (−M) and with (+M) pre-addition of 10 mM MTSEA. (D and H) Uptake of KH2PO4 in phosphate-starved cells of the GigmPT (WT) and Ala146C(D), Val357C, Ile373C, or Thr374C(H) mutants with (+M) and without (−M) pre-addition of 10 mM MTSEA. (E and I) Increase in trehalase activity after supply of 1 mM KH2PO4 to the Ala146C(E) or Val357C(I) mutants without (−M) and with (+M) pre-addition of 10 mM MTSEA in the lack of or existence of 50 mM KH2PO4. (F and J) Uptake of 1 mM KH2PO4 in phosphate-starved cells of the Ala146C(F), Val357C, Ile373C, or Thr374C(J) mutants without (−M) and with (+M) pre-addition of 10 mM MTSEA in the lack of or existence of 50 mM KH2PO4. The SD values are shown; n = 3.

A146 and Val357 Residues Are Required for the Phosphate-Binding Site of GigmPT

To determine which residues are important for phosphate binding, we used site-directed mutagenesis to replace different residues of TMD IV and TMD VIII in GigmPT with cysteines, due to their significant structural similarity to the corresponding regions in the Pho84 sensor, and then tested the transport and signaling activities of the cysteine-substituted mutant proteins (substituted cysteine accessibility method [SCAM]; see Methods). Cysteine substitution of the highly conserved residues rich in glycine (Gly158, Gly160, and Gly162) led to inactive proteins of GigmPT (data not shown).

2-Aminoethyl methanethiosulfonate hydrobromide (MTSEA), a sulfhydryl-binding compound that interacts with the site of water-soluble substrates, was pre-added to estimate transport and signaling functions of the cysteine-substituted GigmPT (Popova et al., 2010). Our data showed that the GigmPTA146C mutant abolished both the trehalase activity and phosphate transport by pre-addition of MTSEA (Figure 8C and 8D), indicating that the residue A146 in GigmPT may be exposed in the substrate-binding site, and the binding of MTSEA to the A146C mutant blocked the binding site. Besides, we carried out a competitive protection experiment to prove that MTSEA and Pi compete for the same substrate-binding site (Popova et al., 2010). The high-concentration Pi and MTSEA were pre-added to yeast carrying GigmPTA146C at the same time. The result showed that transport and signaling functions of GigmPTA146C protein were partially recovered, probably because the binding of phosphate to this site neutralized the binding of MTSEA to the same site (Figure 8E and 8F).

Popova et al. (2010) reported that the residue Val392 in TMD VIII of the Pho84 phosphate transceptor was also required for transport and signaling. Thus, the role of the corresponding residue V357 in TMD VIII of GigmPT was determined using SCAM. The results revealed that the residue GigmPT V357C was also important for phosphate transport and PKA signaling (Figure 8G and 8H). Similarly, the protection experiment showed that both transport and signaling were recovered upon pre-addition of 50 mM phosphate (Figure 8I and 8J). In addition, the residues I373C and T374C were also found to reduce the transport activity, but not PKA signaling (Figure 8H and 8J; Supplemental Figure 15). These data suggested that the residue V357, like the residue A146 in GigmPT, may also be exposed in the phosphate-binding site. The findings that phosphate transport and trehalase activity declined in the GigmPT A146C and GigmPT V357C mutants after addition of MTSEA and that the decline

could be recovered by adding phosphate indicate that GigmPT probably uses the same substrate-binding site for substrate transport and PKA signaling. In addition, it was shown that the Arg154, Asp164, Asp322, and Lys459 are required for GigmPT transport activity but not signaling function (see Supplemental Results).

Discussion

The various nutrient carriers working at both the soil–fungus and fungus–plant interfaces are required for the main nutrient exchange processes in AM symbiosis (Supplemental Figure 19; Bonfante and Genre, 2010). Therefore, PTs that operate in AM fungal and plant symbionts take up phosphate from the soil and transfer it to the host cells, but the molecular mechanisms and regulation of Pi transport and signaling in AM symbiosis remain poorly understood. In this study, we isolated, identified, and functionally characterized a high-affinity phosphate transceptor from the AM fungus G. margarita.

GigmPT Belongs to the High-Affinity Transporter Family and Mediates Pi Acquisition

In AM fungi, transport of Pi across the PM of extraradical hyphae is mediated by known PTs (Supplemental Figure 19), such as GvPT, GintPT, and GmosPT (Harrison and van Buuren, 1995, Benedetto et al., 2005 and Fiorilli et al., 2013). The new results show that G. margarita expresses a phosphate transporter (GigmPT) that is able to transport phosphate (Figure 2). We found that GigmPT functions as a high-affinity transporter for phosphate with a Km of 1.8 ± 0.7 μM (Figure 2D). This Km value is in the range of high-affinity transport reported for the P-uptake systems that were identified in the germ tubes of G. margarita (Thomson et al., 1990). The pH optimum of GigmPT is close to that of MtPT4 located at the PAM (Harrison et al., 2002). GigmPT may mediate phosphate uptake at fungus–soil interface under Pi shortage regarding its transcription in extraradical hyphae (Supplemental Figure 4), and could be functional in AM symbiosis inside the roots regarding transcription of GigmPT during the intraradical phase (Figure 3A and 3B). We further localized GigmPT expression in the arbuscules and intraradical hyphae (Figures 3C and 4), and found that the expression profiling of GigmPT is similar to its homologs, as described previously (Benedetto et al., 2005, Balestrini et al., 2007 and Fiorilli et al., 2013). This finding poses a new question regarding the function of GigmPT at the plant–fungal interface: whether the fungus reabsorbs the Pi from the apoplast or PAS (Fiorilli et al., 2013). Based on the high-affinity property of GigmPT and the localization of GigmPT protein in the arbuscules, we prefer the reabsorption hypothesis whereby GigmPT is in charge of the Pi influx from the apoplast to the fungus (Supplemental Figure 19). However, to make this postulation clearer, further studies concerning the shifts of Pi concentration in the PAS and its effect on the PT genes in the two partners are still necessary. In addition, like the PHO1 and XPR1 acting as Pi exporters in plant and animal (Hamburger et al., 2002 and Giovannini et al., 2013), respectively, the orthologous AM fungal transporters (see Table 1 and Supplemental Figure 20B) responsible for the efflux of Pi to the apoplast also need to be characterized to fully elucidate the regulatory mechanisms of Pi transport at the arbuscule–PAS interface.

Involvement of GigmPT in Carbon–Phosphorus Homeostasis in AM Symbiosis

The transcription of the PTs GigmPT, GigmPT1, and GigmPT2 in G. margarita was regulated in response to carbon besides the regulation by phosphate. Our data showed

that carbon availability induces the expression of GigmPT and GigmPT1 in extraradical mycelia under deficient-Pi conditions and has no effect on transcription of GigmPT under abundant Pi conditions (Supplemental Figure 7). A carbon supply would be expected to accumulate a large amount of carbon skeletons prepared for the syntheses of organic phosphate compounds and nucleic acids, and thus, under Pi shortage, fungal Pi uptake is required for these metabolic processes. In turn, the plants competitively acquire Pi through AsPT1 and AsPT4 genes in AM symbiosis (Supplemental Figure 7D). However, GigmPT was unchanged while GigmPT1 was repressed in intraradical mycelia under normal Pi conditions after carbon supplementation (Supplemental Figure 7A, 7B, and 7F), suggesting tight but opposite control of these genes in IRM and ERM in such a case. This reciprocal regulation is unknown. A possible explanation is that AM fungal cells under this condition obtained more carbohydrate transfer and more Pi to the plant cells regarding the transcription of AM-specific AsPT1 and AsPT4 (Supplemental Figure 7D), rather than retrieved Pi that had been released.

In contrast to the transcription of GigmPT and GigmPT1 genes, GigmPT2 expression was downregulated in both mycelia after the addition of sucrose (Supplemental Figure 7C), revealing that GigmPT2 was negatively regulated by a carbon-dependent signaling pathway. We propose that GigmPT2 is acting as an Msn4/STRE-controlled gene regarding the presence of the STRE element in its promoter (Supplemental Figure 3). A possible explanation is that sucrose availability in Pi-deprived mycelia can rapidly trigger a PKA signaling cascade by the Pi sensor GigmPT (see Supplemental Figures 7 and 20) or unknown nutrient sensors and cause the repression of GigmPT2. Conversely, the transcript profiling of GigmPT2 is derepressed in the GigmPT knockdown lines (Table 1), reinforcing the notion that GigmPT2 is probably regulated by GigmPT. These findings provided new insights into fungal PT gene regulation in AM symbiosis.

Moreover, the Pi concentration and amount of 33P in the roots significantly increased with an increase in sucrose availability (Supplemental Figure 6), implying that the carbon signal could trigger the symbiotic Pi transport to the host. Indeed, Blee and Anderson (1998) proposed that a carbon-based signal from the vascular tissue to the cortical cell may act as a trigger for the development of AM symbiosis. Moreover, increased transfer of Pi from the fungus to the host led to the host boosting radioactive 14C flux to the fungal partner (Supplemental Figure 6B). Taken together, these data implied that GigmPT could be involved in carbon–phosphorus homeostasis in AM symbiosis.

The molecular and physiological aspects of evidence reinforced the proposal that plants reward the fungal symbiont with carbohydrates, and in turn its fungal symbiont enhances cooperation by increasing nutrient transfer to those roots providing more carbohydrates, emphasizing that reciprocal reward stabilizes cooperation in mycorrhizal symbiosis and results in homeostasis of the bidirectional carbon–phosphorus exchange between two symbionts (Kiers et al., 2011). Further studies to determine the carbon-dependent mechanisms of gene regulation in AM fungi will help to define the reciprocal regulatory mechanisms.

GigmPT Is Required for Arbuscular Mycorrhizal Symbiosis

The finding that the inactivation of GigmPT by HIGS leads to fungal growth arrest and impaired arbuscule development of G. margarita shows the significance of this transporter for AM symbiosis. Thus, GigmPT is required for the development of AM symbioses and the activity of AM fungus within roots. Based on a previous study

(Javot et al., 2007), we postulated a model in which phosphate could be an important signal in the regulation of arbuscule development and G. margarita hyphal growth in roots. The phosphate retrieved by GigmPT acts as the signal to ensure the activity of the hyphae and arbuscules during symbiosis. Lacking this Pi signal, the arbuscules are impaired or dead, and growth of the fungus is prevented (Javot et al., 2007). The G. margarita itself needs to reabsorb an amount of Pi from the apoplasmic space to meet demands during fungal growth and division. Furthermore, our functional analysis in yeast revealed that GigmPT encodes a functional Pi transporter in the PM (Figure 2B and 2C), indicating that GigmPT may play a major role in Pi reuptake at the arbuscule–PAS interface. Thus, we can speculate the involvement of GigmPT in fine-tuning Pi homeostasis at the periarbuscular interface dependent on nutrient status within the two symbionts. Under Pi shortage, Pi released is also perceived by the fungal partner; in the presence of Pi, amounts of Pi in PAS are received by plant cells rather than fungal cells, suggesting that the competition of Pi acquisition between two partners may occur in the cells harboring arbuscules. Thus, tight control of GigmPT in arbuscules might be required for this complex mechanism, whereby adequate Pi in PAS is required for the regulation of arbuscules to optimize utilization of the essential nutrient. Upon disruption of GigmPT, arbuscule development was hampered, resulting from deficiencies in signals that coordinate maximal expansion of arbuscules. Interestingly, the transcription of AsPT1 and AsPT4 in GigmPT RNAi roots remained as high as in the control roots, regardless of the status of arbuscules, indicating that expression profiling of AsPT1/4 was indirectly regulated by GigmPT. Thus, the activity of AsPT1/4 genes in GigmPT RNAi roots could account for arbuscule lifespan or symbiotic pathway.

In summary, our data provide insights into the tight regulation of mycorrhizal development and discover a potential mechanism by which the fungus is able to coordinate the AM symbiosis with its nutrient status.

Conservation of PHO and PKA Pathways in AM Fungi and Dual Roles of GigmPT in Phosphate Sensing, Signaling, and Acquisition

It has been demonstrated that transcriptomic sequence is predictive of the PHO and PKA signaling pathways in G. margarita (Salvioli et al., 2016). In brief, the PHO pathway consists of the upstream signaling components (VIP1, IP7, Pho81, Pho80, Pho85, NUC-1, and Pho2) and the downstream transcriptional outputs (Pho5, Pho12, ALP-2, GigmPT1-5), and the PKA pathway is composed of the core signaling cascade (TPK1-3, Bcy1, Rim15, Msn4, and Rap1) and PKA targets (NTH1, TPS2, TSL1, STRE-driven genes, and ribosomal gene) (Table 1). This attempt to understand the phosphate sensing and signaling mechanisms in G. margarita has revealed the presence of common and novel components of the canonical PHO and PKA pathways in this AM fungus. In this study, the comparison of PHO and PKA pathways in R. irregularis and G. margarita (Tisserant et al., 2012, Lin et al., 2014 and Salvioli et al., 2016) further demonstrate that most components are shared between the two species. Comparative transcriptomic analyses of G. margarita and R. irregularis suggest that the core components of the PHO and PKA pathways are highly conserved across glomeraceous AM fungi.

The availability of Pi in rhizosphere or PAS might be sensed in G. margarita by VIP1 and Pho81 genes, whose transcript levels are induced in the symbiotic mycelia grown under Pi-limiting conditions and are repressed in the presence of abundant Pi (Table 1 and Figure 7). It is predicted that intracellular VIP1 and Pho81 proteins transmit the Pi signal downstream of the PHO pathway under low-Pi conditions, and presumed

interaction of Pho81 with IP7 and complex Pho80–Pho85 (Lee et al., 2008 and Secco et al., 2012) permits the nuclear localization of the transcription factor NUC-1, thus activating the PHO-responsive genes (Table 1). In contrast, under normal or excess Pi conditions, expression levels of VIP1 and Pho81 genes are reduced more, the levels of Pho81 protein could decrease in AM fungi, and the active ternary complex Pho81-Pho80-Pho85 may phosphorylate NUC-1 to sequestrate it in the cytoplasm. As a result, the PHO-responsive genes are not activated (Table 1 and Figure 7). However, the transcription of Pho80 and Pho85 is not obviously responsive to the ambient Pi levels (see Table 1), suggesting that the cellular Pi signal is primarily sensed by the VIP1 and Pho81 genes, whose expression levels are largely in response to external Pi levels. However, given that knockdown of GigmPT gene makes the RNAi lines unable to take up ambient Pi or to adequately sense the extracellular Pi signal, in RNAi lines the components of the PHO pathway (VIP1 and Pho81) as well as PHO-responsive genes (Pho5, Pho12, ACP5, ALP-2, and GigmPT1-5) are derepressed compared with the control lines (Table 1 and Figure 7). These data reveal that both the primary signal components and the phosphate-repressible outputs are regulated by GigmPT in such cases, suggesting that Pi signaling is probably functioning downstream of GigmPT.

The repression of GigmPT by HIGS exhibits a series of distinct phenotypes: impaired arbuscules and intraradical hyphae with septa (Figures 5 and 6), derepression of the PHO pathway with regard to transcription of the Pi-repressible genes (Table 1 and Figure 7A–7J), mobilization of polyP as determined by transcription of the polyP metabolism genes (Table 1 and Figure 7K–7N), and repression of the PKA signaling cascade regarding transcription of PKA targets (Table 1 and Figure 7P–7X). It is hypothesized that there exists a positive feedback mechanism in the PHO pathway in G. margarita. We propose that symbiotic mycelia of G. margarita in GigmPT knockdown lines are short of Pi buffer due to very limited polyP. Consequently, AM fungal cells activate their PHO pathway to meet the Pi demands during hyphal growth and arbuscule development, while the putative low-affinity transporters Pho87, Pho90, and Pho91 may be nonfunctional (Supplemental Figure 20A and 20C), resulting in their degradation in vacuoles, and further reducing Pi acquisition or reabsorption. Because the major Pi transporter gene GigmPT is silenced, the mycelia switch to a status in which the PHO pathway is derepressed but Pi acquisition or reabsorption is unremarkable.

In addition, the Msn4-controlled and STRE-driven genes (Table 1) are upregulated in response to limited Pi levels. Contrary to the STRE-driven gene expression profiling, the Rap1-controlled gene RPS13 is repressed under Pi shortage (Figure 7X), suggesting that the transcription rate of PKA targets probably participates in the Pi signaling pathway under these conditions. Thus, it is proposed that the PKA genes (Table 1), especially the TPK genes, are also involved in the Pi signaling pathway during the transcription of PKA targets, whose transcription is modulated in response to external Pi levels. Indeed, GigmPT knockdown reveals a set of genes representing PKA targets that are derepressed or repressed in RNAi lines (Figure 7P–7X), for instance, activation of trehalose metabolism-related genes (NTH1, TPS2, and TSL1) and STRE-driven genes and repression of ribosomal protein gene RPS13, reinforcing the notion that GigmPT primarily senses the extracellular Pi signal after which the PKA protein transmits the signal downstream of the PKA signaling cascade.

Since reduction of the GigmPT gene of G. margarita during AM symbiosis has been shown to inactivate PKA signaling regarding a response in PKA targets, interestingly the STRE-controlled transcription of the trehalase gene NTH1 strongly increases

(Figure 7P), as opposed to the previously observed levels of trehalase activity in yeast experiments (Supplemental Table 2 and Figure 8A), revealing that there exists a tight but opposite regulation of trehalase NTH1 at the transcriptional and post-translational levels in G. margarita (Supplemental Figure 20B and 20D). Like S. cerevisiae (Thevelein, 1996), it is considered that the trehalase activity in AM fungi is also regulated by PKA-driven phosphorylation. Contrary to the drop in enzyme activity of NTH1 in Pi-deprived yeast cells (Figure 8A), the expression of NTH1 gene is obviously induced in the absence of Pi (Figure 7P). It could be that AM fungi express a great deal of NTH1 in the form of inactive enzyme in the case where they synthesize a large amount of trehalose by Msn4-dependent expression of the trehalose synthase complex TPS2 (Figure 7Q and Supplemental Figure 20). The probable explanation for this reciprocal regulation is that AM fungi prepare for states that need to rapidly mobilize the trehalose, such as the readdition of abundant Pi in the media.
Interestingly, in this study the readdition of phosphate or nontransported phosphate-containing compounds such as Gly3P to the phosphate-starved yeast cells expressing GigmPT could trigger PKA signaling, and resulted in activation of trehalase to mobilize trehalose (Supplemental Table 2 and Figure 8A), reinforcing that GigmPT served as a phosphate receptor regarding the presence of the signaling function without transport. However, the competitive inhibitor PAA of phosphate transport via GigmPT could not upregulate the PKA pathway (Figure 8B and Supplemental Figure 14). These results agreed with those previously reported by Popova et al. (2010), indicating that a conformational change after specific substrate binding is required for the PKA signaling cascade via GigmPT, whereas a complete transport cycle of this substrate is not required for PKA signaling via GigmPT. This hypothesis was consistent with the model proposed by Pedersen et al. (2013) for the Pi transport mechanism of PiPT. We identified A146 and V357 as residues that might be exposed to the phosphate-binding site in the GigmPT by using SCAM, as in PHO84 sensor. In both GigmPT and PHO84, mutation of these residues led to decline in functions of the transceptors, indicating that they used the same phosphate-binding site for transport and signaling (Popova et al., 2010). The competition experiment offered powerful evidence for this conclusion. In a subsequent experiment, based on the 3D structure of GigmPT, whose structure was constructed using GlpT, PiPT, and PHO84 permeases as templates from E. coli, P. indica, and S. cerevisiae, respectively (see Figure 1 and Supplemental Figure 16), four residues (R154, D164, D322, and K459) were identified to play a major role in transport but not signaling (Supplemental Figure 17). Therefore, the phosphate sensor GigmPT provided potential evidence that Pi transceptors, including Pho84 sensor, appeared to use the same site for phosphate transport and PKA signaling. However, the two functions are independent and separate during transportation (the mechanisms are detailed in Supplemental Figure 18). In general, we confirmed and extended the mechanisms of recognition and transport through the GigmPT sensor according to phosphate transceptors in eukaryotic cells (Popova et al., 2010, Samyn et al., 2012 and Pedersen et al., 2013). These data provided new insights into the transport and signaling functions of the GigmPT transceptor in fungal cells. On the basis of the aforementioned data, we also propose the hypothesis that depletion and repletion of nutrients (P or C) affect a common PKA pathway (Conrad et al., 2014) in response to conditions that promoted AM fungal growth and development.
In the first version of the scheme for Pi sensing and signaling networks, it has been proposed that GigmPT protein is predominantly located in ERM, arbuscules, and intraradical hyphae in G. margarita (Figure 9), and that GigmPT is functional in the

PHO pathway in the absence of Pi (Supplemental Figure 20A and 20C) and is inactive under abundant Pi conditions regarding transcription of Pi-repressible genes, while GigmPT is functional in the PKA signaling cascade in the presence of Pi regarding a response in PKA targets (Supplemental Figure 20B and 20D). The description of the depiction is detailed in Supplemental Results. Thus, GigmPT is proposed to be the main Pi sensor in G. margarita, being involved in Pi acquisition from rhizosphere or Pi reabsorption from PAS via upregulation of the PHO pathway as well as by sensing extracellular Pi changes through the activation of the PKA signaling cascade.

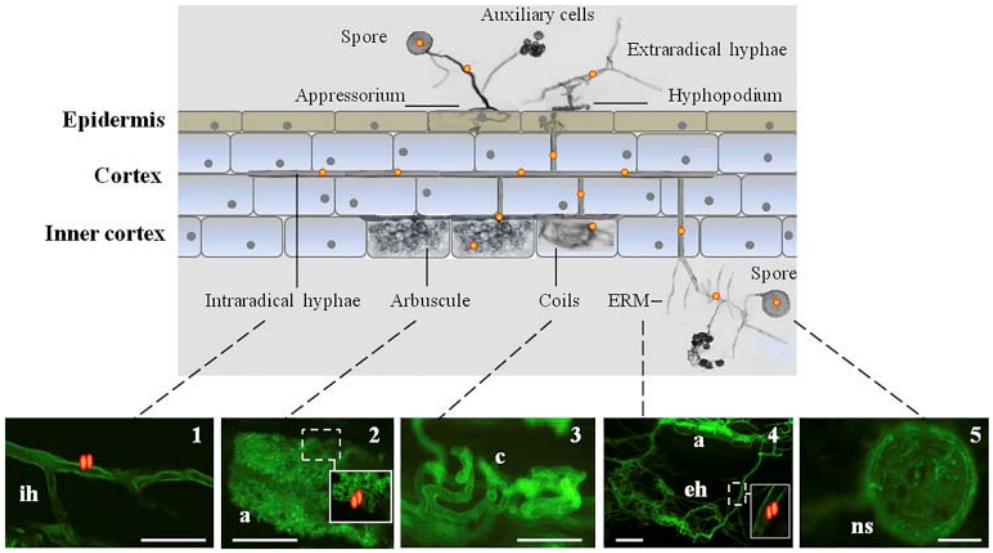

Figure 9. Proposed Working Model of GigmPT in G. margarita.
Graphical representation of the symbiotic structures of G. margarita and the localizations of GigmPT gene (yellow circles) and its protein (yellow double ovals). The dual roles of GigmPT in the acquisition and reabsorption of phosphate from rhizosphere and periarbuscular space during symbiosis (see Supplemental Figure 20). The uptake and reuptake of phosphate that occur in ERM and IRM possibly involve the same phosphate transporter of G. margarita. In ERM, phosphate is absorbed by GigmPT that is expressed in extraradical hyphae (yellow circles) and probably localized on the membrane of extraradical hyphae (yellow double ovals). In IRM, phosphate is reabsorbed through GigmPT that is localized on the PM of arbuscules and intraradical hyphae (yellow double ovals). Importantly, it is proposed that GigmPT functions as a Pi sensor (or transceptor) in the regulation of putative PHO and PKA signaling cascades during AM symbiosis (see Supplemental Figure 20): GigmPT acts as Pi transporter in view of the transcription of PHO-responsive genes under Pi deficiency and serves as Pi receptor regarding a response in PKA targets under Pi-sufficient conditions. The images 1–5 represent various AM fungal tissues from WGA–488 staining. ih, intraradical hyphae; a, arbuscule; c, coils; ERM, extraradical mycelium; eh, extraradical hyphae; ns, new spore. Scale bars represent 50 μm (1 and 2), 100 μm (3), and 250 μm (4 and 5).

Further studies, such as characterizing the precise roles of the novel Pi transporter genes identified in this work, validating the protein–protein interactions in both PHO and PKA pathways and the biochemical functions of core components of both pathways, and determining the direct evidence of PKA-dependent mechanisms in G. margarita, are needed to define the underlying Pi sensing and signaling mechanisms. In addition, the RNA-seq data analysis coupled with gene expression profiling show that both G. margarita and Gigaspora rosea consist of multiple distinct SPX domain-containing proteins (Salvioli et al., 2016 and Tang et al., 2016), indicative of the existence of potential Pi sensors in AM fungi to respond to cellular Pi levels through binding inositol polyphosphate in eukaryotes (Wild et al., 2016) and adapting to fluctuation of available phosphate. Thus, a major goal in this field will be to unravel a

potential master cellular Pi sensor controlling AM fungal Pi homeostasis during symbiosis.

Methods

Biological Materials

The AM fungus Gigaspora margarita (BEG34) used in this work was kindly provided by the International Bank of Glomeromycota (Dijon, France). G. margarita was employed to inoculate the roots of Astragalus sinicus L. as described elsewhere (Xie et al., 2013). Spores of G. margarita were produced in pot system on A. sinicus and collected by wet sieving, after which the spores were soaked in 2% Chloramine T (Sigma-Aldrich, St. Louis, MO, USA) for 15 min, washed at least three times in sterile water, and immersed in a mixture of antibiotic solution containing 200 mg l−1 streptomycin and 100 mg l−1 gentamycin (Sigma-Aldrich) for 10 min. After washing in sterile water, spores were immediately frozen in liquid nitrogen and stored at −70°C before use. For preparation of germinating spores, about 400 surface-sterilized G. margarita spores were placed in sterile H2O and incubated in the dark for 10 days at 26°C to induce germination. ERM of G. margarita was produced in the bicompartmental system (Maldonado-Mendoza et al., 2001).

R. irregularis DAOM 197198 was used in this study to clone the GiPT2 and GiPT4 genes, which encode two low-affinity Pi transporters the Na+/Pi symporter Pho87p and Pho91p, respectively (Tisserant et al., 2012 and Lin et al., 2014). Saccharomyces cerevisiae strain S288C was employed for the isolation of Pi sensor gene pho84. Plant materials and growth conditions are provided in Supplemental Materials and Methods.

Phosphate or Sucrose Treatments of Mycorrhizal Roots

In the pot system, the roots of A. sinicus colonized with G. margarita BEG34 were maintained in low-P condition (6.70 mg P kg−1). After 2 weeks, the mycorrhizal plants were supplied with Hoagland's nutrient solution containing 0.065 mM KH2PO4 (low-P treatment), 0.2 mM KH2PO4 (moderate-P treatment), or 1 mM KH2PO4 (high-P treatment). Plants were harvested at 4 weeks post inoculation (wpi). For AM monoxenic cultures, A. sinicus hairy roots were mycorrhized with G. margarita on MSR medium containing 30 μM KH2PO4. After 4 weeks, a part of the mycorrhizal roots was transferred to fresh MSR medium containing 0, 3, 30, or 300 μM KH2PO4, and roots were harvested after 2 weeks of incubation at 26°C in the dark; other parts of mycorrhizal roots were transferred to the bicompartmental system, and treated with 10 ml of MSR medium containing 3 μM or 300 μM KH2PO4 in the hyphal compartment. ERM and IRM were obtained after 42 or 50 days of incubation at 26°C in the dark.

The sucrose- and phosphate-treatment experiments were performed as described in Supplemental Materials and Methods. The mycelia were collected with dissecting forceps, after which all the materials were rinsed in sterile dH2O and dried with filter paper, immediately frozen in liquid nitrogen, and stored at −70°C until use.

Cloning of Genomic DNA and cDNA for G. margarita Phosphate Transporter

A pair of degenerate primers (see Supplemental Table 3) was designed based on the amino acid sequences of highly conserved regions within the PTs of G. versiforme, R. irregularis, F. mosseae, Piriformospora indica (Yadav et al., 2010), S. cerevisiae, Pholiota nameko (Tasaki et al., 2002), and Magnaporthe grisea. Subsequent PCR on the total DNA from G. margarita spores resulted in a 1131-bp amplified DNA

segment encoding a putative Pi transporter, namely GigmPT. The 5′ and 3′ regions of the GigmPT gene were isolated by thermal asymmetric interlaced PCR (Liu and Chen, 2007) and inverse PCR (Sambrook and Russell, 2006). A phosphate transporter gene-specific fragment was amplified by RT–PCR using the degenerate primers and the mRNA isolated from G. margarita mycorrhizal roots 4 weeks after inoculation. This cDNA fragment was lengthened with 5′- and 3′-RACE (rapid amplification of cDNA ends) (Scotto-Lavino et al., 2006a and Scotto-Lavino et al., 2006b).

Southern Blot Analysis

The total DNA was isolated from G. margarita spores as described by Zézé et al. (1994). Southern blotting for GigmPT gene was performed according to the previous work (Xie et al., 2013).

RNA Isolation, First-Strand cDNA Synthesis, and Quantitative Real-Time PCR

Total RNA was isolated from the different tissues of G. margarita with TRIzol reagents (Invitrogen) following the manufacturer's protocol. The first-strand cDNA synthesis, RT–PCR, and real-time RT–PCR were performed as reported previously (Zhang et al., 2010), and the actin gene of G. margarita was used as the internal standard. Real-time qRT–PCR analysis of the selected genes possibly involved in the phosphorus-sensing network was further performed to validate the data derived from the RNA-seq experiment (Salvioli et al., 2016). Details of the procedures are provided in Supplemental Materials and Methods. The gene-specific primers and corresponding sequences are listed in Supplemental Table 5.

RNA-Sequencing Data Analysis

The G. margarita BEG34 transcriptome shotgun assembly data were deposited at GenBank in the NCBI (Salvioli et al., 2016). Functional annotation followed the Gene Ontology (Ashburner et al., 2000) and G. margarita Transcriptome Database (Salvioli et al., 2016). Using the MeV (MultiExperiment Viewer, v4.9) software, DESeq2-normalized expression data (Salvioli et al., 2016) were plotted in heatmaps for comparison. Data analyses are detailed in Supplemental Materials and Methods.

Localization of GigmPT in Yeast Cells

The subcellular localization of GigmPT in yeast was examined with a C-terminal fusion of GigmPT to GFP in the yeast strain as described by Xie et al. (2013). The image capture was performed using a fluorescence microscope (Olympus BX51, Japan).

The coexpression of GigmPT and PHO84 proteins was performed as described in Supplemental Materials and Methods. The two fluorescent signals were observed with a Zeiss LSM 510 confocal microscope.

Yeast Complementation

Complementation in yeast was performed as described previously (Daram et al., 1999 and Ai et al., 2009). The acid phosphatase (rAPase) was determined as described by Yadav et al. (2010).

Uptake Studies with Radioactive Orthophosphate

To determine the kinetic properties of the phosphate transporter GigmPT, we performed uptake experiments using 32Pi with the positive yeast transformants (Ai et al., 2009 and Yadav et al., 2010). The inhibition and competition of 32Pi uptake

studies were performed according to a previous publication (Popova et al., 2010). Samples were measured in a scintillation counter (1450 MicroBeta Trilux LSC).

In Situ Hybridization of Mycorrhizal Roots

In situ hybridization was performed as described previously (Kouchi and Hata, 1993 and Daram et al., 1999). The digoxigenin-labeled (Roche) probes were synthesized from the 3′ end cDNA of GigmPT.

Antibody Preparation and Immunolocalization of GigmPT

Antibodies specific for the GigmPT-driven peptides were produced in rabbits. The antibodies were against a peptide corresponding to the N-terminal 15 amino acids of the GigmPT protein (5′-NIVIEDNDYDKRRRE-3′) predicted to a nonconserved region in this protein. The serum was analyzed for the presence of anti-GigmPT antibodies that recognized the peptide by ELISA analysis. A 1:500 dilution of the antibodies was prepared for immunolocalization analysis.

Immunolocalization was performed as described in Garcia et al., 2013 and Pérez-Tienda et al., 2011, and Harrison et al. (2002) with some modifications. The protocol is detailed in Supplemental Materials and Methods.

Host-Induced Gene Silencing

HIGS was carried out as described previously (Helber et al., 2011). For GigmPT silencing by the host, 305 bp of the GigmPT cDNA at 5′ end was cloned using the specific primers GigmPTdsF1 and GigmPTdsR1 and introduced into the RNAi vector pDS1301(Chu et al., 2006). The GigmPT RNAi construct was used to generate A. sinicus hairy roots by Agrobacterium rhizogenes transformation as described by Li et al. (2008). The EV control and RNAi A. sinicus hairy roots were subsequently inoculated with G. margarita and the colonization was detected at 28 days post inoculation (dpi). Similar to the hairy root generation, the composite plants with hairy roots (n > 15 lines: RNAi roots > 15 lines; control roots > 15 lines) were obtained by A. rhizogenes transformation. The selected plants or hairy roots carrying RNAi vector were inoculated with G. margarita. The parts of NM and AM roots were used to validate the presence of hairpin construct and siRNA, whereas ERM was collected to detect the siRNA levels. The parts of AM roots were harvested at 4 wpi for acid fuchsin (for hairy roots) or WGA488 (for composite plants) staining, and other parts were collected for subsequent gene expression analysis.

siRNA Analysis

RNA assays were carried out according to the Digoxigenin Application Manual for Hybridization from Roche. RNA gel blot was carried out as described previously (Helber et al., 2011). The analysis of siRNAs derived from GigmPT was performed as previously described (Nicolás et al., 2003 and Pall and Hamilton, 2008).

Quantification of Mycorrhizal Colonization

Mycorrhizal roots were detected with acid fuchsin or WGA488 staining, and colonization was quantified with the program MYCOCALC as described previously (Trouvelot, 1986). Images of mycorrhizal roots stained with acid fuchsin were taken with a confocal microscope (Olympus), while images of mycorrhizal roots stained with WGA488 were taken with a fluorescence microscope (Olympus BX51).

Histochemical Staining
For the detection of A. sinicus hairy roots, histochemical β-glucuronidase assays were performed as described previously (Scarpella et al., 2003). The earlier publications were followed for ALP (Zhao et al., 1997) and polyphosphate (PolyPi) (Ezawa et al., 2003) staining.

Experimental Design for Radioactive Sucrose and Phosphate Transfer
The effect of sucrose availability on Pi transfer through G. margarita was detected using [U-14C]sucrose (PerkinElmer, USA). Zero, 3 mM, 30 mM, or 90 mM radioactive [U-14C]sucrose (specific activity of 100 mCi mM−1) was supplied to the RHC. Meanwhile, 30 μM 33P-labeled H3PO4 (PerkinElmer) was added to the HC. After 2 weeks, the roots and the ERM of the HC and RHC were harvested and prepared for further analysis. P and C transport were measured under different C supply conditions by adding 0, 3, 30, or 90 mM [U-14C]sucrose to the RHC when the 30 μM 33P-labeled H3PO4 (specific activity 250 mCi mM−1) was supplied. The 14C and 33P were measured with the 1450 MicroBeta Trilux LSC (PerkinElmer) and LS 6500 Multi-Purpose scintillation counters, respectively.

Analysis of Phosphate Pool Distribution
The phosphate pools in mycorrhizal roots were extracted according to the method described previously (Fellbaum et al., 2012).

In Silico Analysis and Homology Modeling
In silico analysis of the GigmPT gene sequence was calculated using the following tools and software. The BLAST program was used for homology prediction at the NCBI site (www.ncbi.nlm.nih.gov), and MULTIALIN for multiple sequence alignment of AM fungal PT proteins. The functional motifs in GigmPT were predicted using the PROSITE database (http://www.expasy.ch/prosite/). The promoter sequence analysis was performed for the existence of cis-activated elements using the tools available from The Promoter Database of S. cerevisiae (SCPD) (http://rulai.cshl.edu/SCPD/; Zhu and Zhang, 1999). The homology modeling for GigmPT TMDs was constructed as previously reported by Yadav et al. (2010). The structure of GlPT from E. coli and PiPT from P. indica was used as the template for homology modeling (Eswar et al., 2003, Huang et al., 2003 and Pedersen et al., 2013).

Yeast Strain Growth and Phosphate Starvation Conditions
Yeast growth and phosphate starvation were performed as described previously (Popova et al., 2010).

Phosphate Transport and Trehalase Activity Determination
Phosphate uptake was assayed by means of radioactively labeled 32Pi (Perkin Elmer), and the determination of trehalase activity was performed as described previously (Pernambuco et al., 1996 and Popova et al., 2010).

Substituted Cysteine Accessibility Method Analysis
Analysis of SCAM was carried out as described by Popova et al. (2010). The site-directed mutagenesis kit (Beyotime, China) was used for SCAM studies. MTSEA (10 mM) was used for phosphate transport and trehalase activity assays. Oligonucleotides used for site-directed mutagenesis are provided in Supplemental Table 4.

Phylogenetic Analysis
Phylogenetic trees were constructed using MEGA v4.1 phylogeny software. The multiple sequence alignment was performed by ClustalW, and the neighbor-joining method was applied for the construction of the phylogeny. Bootstrap tests were performed using 1000 replicates. Accession numbers of the predicted proteins are given in Supplemental Material and Methods.

Statistical Analyses
The data were assayed by analysis of variance (SPSS 16.0 software). All experiments in yeast were repeated three times, and all parameters and calculated variables were tested for differences between treatments and their respective controls using Turkey's honest significant difference test. Differences are described as significant and marked with asterisks with for values of $*P < 0.05$ and $**P < 0.01$. Data represent the mean ± SD of independent replicates.

Funding
This work was supported by grants from the National Natural Science Foundation of China (grant no. 30870082 and grant no. 31270159).

Acknowledgments
We thank Professor Guohua Xu for providing the yeast mutant strains and plasmid, Professor Shiping Wang for providing the pDS1301 vector for the HIGS experiment, Professor Zhongming Zhang for providing strain K599 for the plant transformations, and Jianyong An and Qianming Zheng for help with the experiments of the radioactive uptake. We would like to thank Jennifer Mach, Ph.D. for revising the manuscript. No conflict of interest declared.

References
P. Ai, S. Sun, J. Zhao, X. Fan, W. Xin, Q. Guo, L. Yu, Q. Shen, P. Wu, A.J. Miller, et al. Two rice phosphate transporters, OsPht1;2 and OsPht1;6, have different functions and kinetic properties in uptake and translocation Plant J., 57 (2009), pp. 798–809

T. Aono, I.E. Maldonado-Mendoza, G.R. Dewbre, M.J. Harrison, M. Saito Expression of alkaline phosphatase genes in arbuscular mycorrhizas New Phytol., 162 (2004), pp. 525–534

M. Ashburner, C.A. Ball, J.A. Blake, D. Botstein, H. Butler, J.M. Cherry, A.P. Davis, K. Dolinski, S.S. Dwight, J.T. Eppig, et al. Gene ontology: tool for the unification of biology. The Gene Ontology Consortium Nat. Genet., 25 (2000), pp. 25–29

R. Balestrini, J. Gómez-Ariza, L. Lanfranco, P. Bonfante Laser microdissection reveals that transcripts for five plant and one fungal phosphate transporter genes are contemporaneously present in arbusculated cells Mol. Plant Microbe Interact., 20 (2007), pp. 1055–1062

A. Benedetto, F. Magurno, P. Bonfante, L. Lanfranco Expression profiles of a phosphate transporter gene (GmosPT) from the endomycorrhizal fungus Glomus mosseae Mycorrhiza, 15 (2005), pp. 620–627

K.A. Blee, A.J. Anderson Regulation of arbuscule formation by carbon in the plant Plant J., 16 (1998), pp. 523–530

P. Bonfante, A. Genre Mechanisms underlying beneficial plant-fungus interactions in mycorrhizal symbiosis Nat. Commun., 1 (2010), p. 48

M. Bucher, S. Wegmüller, D. Drissner Chasing the structures of small molecules in arbuscular mycorrhizal signaling Curr. Opin. Plant Biol., 12 (2009), pp. 500–507

M. Bun-Ya, M. Nishimura, S. Harashima, Y. Oshima The PHO84 gene of Saccharomyces cerevisiae encodes an inorganic phosphate transporter Mol. Cell. Biol., 11 (1991), pp. 3229–3238

Z. Chu, M. Yuan, J. Yao, X. Ge, B. Yuan, C. Xu, X. Li, B. Fu, Z. Li, J.L. Bennetzen, et al. Promoter mutations of an essential gene for pollen development result in disease resistance in rice Genes Dev., 20 (2006), pp. 1250–1255

M. Conrad, J. Schothorst, H.N. Kankipati, G.V. Zeebroeck, M. Rubio-Texeira, J.M. Thevelein Nutrient sensing and signaling in the yeast Saccharomyces cerevisiae FEMS Microbiol. Rev., 38 (2014), pp. 254–299

G. Cox, K.J. Moran, F. Sanders, C. Nockolds, P.B. Tinker Translocation and transfer of nutrients in vesicular-arbuscular mycorrhizas. III. Polyphosphate granules and phosphorus translocation New Phytol., 84 (1980), pp. 649–659

P. Daram, S. Brunner, C. Rausch, C. Steiner, N. Amrhein, M. Bucher Pht2;1 encodes a low-affinity phosphate transporter from Arabidopsis Plant Cell, 11 (1999), pp. 2153–2166

N. Eswar, B. John, N. Mirkovic, A. Fiser, V.A. Ilyin, U. Pieper, A.C. Stuart, M.A. Marti-Renom, M.S. Madhusudhan, B. Yerkovich, et al. Tools for comparative protein structure modeling and analysis Nucleic Acids Res., 31 (2003), pp. 3375–3380

T. Ezawa, T.R. Cavagnaro, S.E. Smith, F.A. Smith, R. Ohtomo Rapid accumulation of polyphosphate in extraradical hyphae of an arbuscular mycorrhizal fungus as revealed by histochemistry and a polyphosphate kinase/luciferase system New Phytol., 161 (2003), pp. 387–392

C.R. Fellbaum, E.W. Gachomo, Y. Beesetty, S. Choudhari, G.D. Strahan, P.E. Pfeffer, E.T. Kiers, H. Bücking Carbon availability triggers fungal nitrogen uptake and transport in arbuscular mycorrhizal symbiosis Proc. Natl. Acad. Sci. USA, 109 (2012), pp. 2666–2671

R.D. Finlay Ecological aspects of mycorrhizal symbiosis: with special emphasis on the functional diversity of interactions involving the extraradical mycelium J. Exp. Bot., 59 (2008), pp. 1115–1126

V. Fiorilli, L. Lanfranco, P. Bonfante The expression of GintPT, the phosphate transporter of Rhizophagus irregularis, depends on the symbiotic status and phosphate availability Planta, 237 (2013), pp. 1267–1277

A.H. Fitter What is the link between carbon and phosphorus fluxes in arbuscular mycorrhizas? A null hypothesis for symbiotic function New Phytol., 172 (2006), pp. 3–6

K. Garcia, M.Z. Haider, A. Delteil, C. Corratgé-Faillie, G. Conéjero, M. Tatry, A. Becquer, L. Amenc, H. Sentenac, C. Plassard, et al. Promoter-dependent expression of the fungal transporter HcPT1.1 under Pi shortage and its spatial localization in ectomycorrhiza Fungal Genet. Biol., 58-59 (2013), pp. 53–61

F. Giots, M. Donaton, J. Thevelein Inorganic phosphate is sensed by specific phosphate carriers and acts in concert with glucose as a nutrient signal for activation of the protein kinase A pathway in the yeast Saccharomyces cerevisiae Mol. Microbiol., 47 (2003), pp. 1163–1181

D. Giovannini, J. Touhami, P. Charnet, M. Sitbon, J.L. Battini Inorganic phosphate export by the retrovirus receptor XPR1 in metazoans
Cell Rep., 3 (2013), pp. 1866–1873
A. Gojon, G. Krouk, F. Perrine-Walker, E. Laugier Nitrate transceptor(s) in plants J. Exp. Bot., 62 (2011), pp. 2299–2308

C. Gutjahr, M. Parniske Cell and developmental biology of arbuscular mycorrhiza symbiosis Annu. Rev. Cell Dev. Biol., 29 (2013), pp. 593–617

D. Hamburger, E. Rezzonico, J. MacDonald-Comber Petetot, C. Somerville, Y. Poirier Identification and characterization of the Arabidopsis PHO1 gene involved in phosphate loading to the xylem Plant Cell, 14 (2002), pp. 889–902

M.J. Harrison Molecular and cellular aspects of the arbuscular mycorrhizal symbiosis Annu. Rev. Plant Physiol. Plant Mol. Biol., 50 (1999), pp. 361–389

M.J. Harrison Signaling in the arbuscular mycorrhizal symbiosis Annu. Rev. Microbiol., 59 (2005), pp. 19–42

M.J. Harrison, M.L. van Buuren A phosphate transporter from the mycorrhizal fungus Glomus versiforme Nature, 378 (1995), pp. 626–629

M.J. Harrison, G.R. Dewbre, J. Liu A phosphate transporter from Medicago truncatula involved in the acquisition of phosphate released by arbuscular mycorrhizal fungi Plant Cell, 14 (2002), pp. 2413–2429

N. Helber, K. Wippel, N. Sauer, S. Schaarschmidt, B. Hause, N. Requena A versatile monosaccharide transporter that operates in the arbuscular mycorrhizal fungus Glomus sp is crucial for the symbiotic relationship with plants Plant Cell, 23 (2011), pp. 3812–3823

C.H. Ho, S.H. Lin, H.C. Hu, Y.F. Tsay CHL1 functions as a nitrate sensor in plants Cell, 138 (2009), pp. 1184–1194

Y. Huang, M.J. Lemieux, J. Song, M. Auer, D.N. Wang Structure and mechanism of the glycerol-3-phosphate transporter from Escherichia coli Science, 301 (2003), pp. 616–620

H.C. Hürlimann, M. Stadler-Waibel, T.P. Werner, F.M. Freimoser Pho91 is a vacuolar phosphate transporter that regulates phosphate and polyphosphate metabolism in Saccharomyces cerevisiae Mol. Biol. Cell, 18 (2007), pp. 4438–4445

H.C. Hürlimann, B. Pinson, M. Stadler-Waibel, S.C. Zeeman, F.M. Freimoser The SPX domain of the yeast low-affinity phosphate transporter Pho90 regulates transport activity EMBO Rep., 10 (2009), pp. 1003–1008

I. Jakobsen, L.K. Abbott, A.D. Robson External hyphae of vesicular-arbuscular mycorrhizal fungi associated with Trifolium subterraneum L. 2: hyphal transport of 32P over defined distances New Phytol., 120 (1992), pp. 509–516

H. Javot, R.V. Penmetsa, N. Terzaghi, D.R. Cook, M.J. Harrison A Medicago truncatula phosphate transporter indispensable for the arbuscular mycorrhizal symbiosis Proc. Natl. Acad. Sci. USA, 104 (2007), pp. 1720–1725

E.T. Kiers, M. Duhamel, Y. Beesetty, J.A. Mensah, O. Franken, E. Verbruggen, C.R. Fellbaum, G.A. Kowalchuk, M.M. Hart, A. Bago, et al. Reciprocal rewards stabilize cooperation in the mycorrhizal symbiosis Science, 333 (2011), pp. 880–882

H. Kouchi, S. Hata Isolation and characterization of novel nodulin cDNAs representing genes expressed at early stages of soybean nodule development Mol. Gen. Genet., 238 (1993), pp. 106–119

Y.S. Lee, H. Huang, F. Quiocho, E. O'Shea Molecular basis of cyclin-CDK-CKI regulation by reversible binding of an inositol pyrophosphate Nat. Chem. Biol., 4 (2008), pp. 25–32

Y. Li, L. Zhou, D. Chen, X. Tan, L. Lei, J. Zhou A nodule-specific plant cysteine proteinase, AsNODF32, is involved in nodule senescence and nitrogen fixation activity of the green manure legume Astragalus sinicus New Phytol., 180 (2008), pp. 185–192

T. Li, Y. Hu, Z. Hao, H. Li, Y. Wang, B. Chen First cloning and characterization of two functional aquaporin genes from an arbuscular mycorrhizal fungus Glomus intraradices New Phytol., 197 (2013), pp. 617–630

K. Lin, E. Limpens, Z. Zhang, S. Ivanov, D.G.O. Saunders, D. Mu, E. Pang, H. Cao, H. Cha, T. Lin, et al. Single nucleus genome sequencing reveals high similarity among nuclei of an endomycorrhizal fungus PLoS Genet., 10 (2014), p. e1004078

Y. Liu, Y. Chen High-efficiency thermal asymmetric interlaced PCR for amplification of unknown flanking sequences Biotechniques, 43 (2007), pp. 649–656

V. Loth-Pereda, E. Orsini, P.E. Courty, F. Lota, A. Kohler, L. Diss, D. Blaudez, M. Chalot, U. Nehls, Bucher, et al. Structure and expression profile of the phosphate Pht1

transporter gene family in mycorrhizal Populus trichocarpa Plant Physiol., 156 (2011), pp. 2141–2154

I.E. Maldonado-Mendoza, G.R. Dewbre, M.J. Harrison A phosphate transporter gene from the extraradical mycelium of an arbuscular mycorrhizal fungus Glomus intraradices is regulated in response to phosphate in the environment Mol. Plant Microbe Interact., 14 (2001), pp. 1140–1148

F.E. Nicolás, S. Torres-Martínez, R.M. Ruiz-Vázquez Two classes of small antisense RNAs in fungal RNA silencing triggered by non-integrative transgenes EMBO J., 22 (2003), pp. 3983–3991

D. Nowara, A. Gay, C. Lacomme, J. Shaw, C. Ridout, D. Douchkov, G. Hensel, J. Kumlehn, P. Schweizer HIGS: host induced gene silencing in the obligate biotrophic fungal pathogen Blumeria graminis Plant Cell, 22 (2010), pp. 3130–3141

G.S. Pall, A.J. Hamilton Improved northern blot method for enhanced detection of small RNA Nat. Protoc., 3 (2008), pp. 1077–1084

M. Parniske Arbuscular mycorrhiza: the mother of plant root endosymbioses Nat. Rev. Microbiol., 6 (2008), pp. 763–775

U. Paszkowski A journey through signaling in arbuscular mycorrhizal symbioses New Phytol., 172 (2006), pp. 35–46

B.P. Pedersen, H. Kumar, A.B. Waight, A.J. Risenmay, Z. Roe-Zurz, B.H. Chau, A. Schlessinger, M. Bonomi, W. Harries, A. Sali, et al. Crystal structure of a eukaryotic phosphate transporter Nature, 496 (2013), pp. 533–536

J. Pérez-Tienda, P.S. Testillano, R. Balestrini, V. Fiorilli, C. Azcón-Aguilar, N. Ferrol GintAMT2, a new member of the ammonium transporter family in the arbuscular mycorrhizal fungus Glomus intraradices Fungal Genet. Biol., 48 (2011), pp. 1044–1055

M.B. Pernambuco, J. Winderickx, M. Crauwels, G. Griffioen, W.H. Mager, J.M. Thevelein Glucose-triggered signalling in Saccharomyces cerevisiae: different requirements for sugar phosphorylation between cells grown on glucose and those grown on non-fermentable carbon sources Microbiology, 142 (1996), pp. 1775–1782

Y. Popova, P. Thayumanavan, E. Lonati, M. Agrochão, J.M. Thevelein Transport and signaling through the phosphate-binding site of the yeast Pho84 phosphate transceptor Proc. Natl. Acad. Sci. USA, 107 (2010), pp. 2890–2895

C. Rausch, P. Daram, S. Brunner, J. Jansa, M. Laloi, G. Leggewie, N. Amrhein, M. Bucher A phosphate transporter expressed in arbuscule-containing cells in potato Nature, 414 (2001), pp. 462–470

W. Remy, T.N. Taylor, H. Hass, H. Kerp Four hundred million-year-old vesicular arbuscular mycorrhizae Proc. Natl. Acad. Sci. USA, 91 (1994), pp. 11841–11843

A. Salvioli, S. Ghignone, M. Novero, L. Navazio, F. Venice, P. Bagnaresi, P. Bonfante Symbiosis with an endobacterium increases the fitness of a mycorrhizal fungus, raising its bioenergetic potential ISME J., 10 (2016), pp. 130–144

J. Sambrook, D.W. Russell Inverse PCR Cold Spring Harb. Protoc. (2006) http://dx.doi.org/10.1101/pdb. prot3487

D.R. Samyn, L. Ruiz-Pávon, M.R. Andersson, Y. Popova, J.M. Thevelein, B.L. Persson Mutational analysis of putative phosphate- and proton-binding sites in the Saccharomyces cerevisiae Pho84 phosphate: H+ transceptor and its effect on signalling to the PKA and PHO pathways Biochem. J., 445 (2012), pp. 413–422

I.R. Sanders Evolutionary genetics: no sex please, we're fungi Nature, 399 (1999), pp. 737–739

E. Scarpella, S. Rueb, A.H. Meijer The RADICLELESS1 gene is required for vascular pattern formation in rice Development, 130 (2003), pp. 645–658

A. Schüßler, D. Schwarzott, C. Walker A new fungal phylum, the Glomeromycota: phylogeny and evolution Mycol. Res., 105 (2001), pp. 1413–1421

E. Scotto-Lavino, G. Du, M.A. Frohman 5' end cDNA amplification using classic RACE Nat. Protoc., 1 (2006), pp. 2555–2562

E. Scotto-Lavino, G. Du, M.A. Frohman 3' end cDNA amplification using classic RACE Nat. Protoc., 1 (2006), pp. 2742–2745

D. Secco, C. Wang, H. Shou, J. Whelan Phosphate homeostasis in the yeast Saccharomyces cerevisiae, the key role of the SPX domain-containing proteins FEBS Lett., 586 (2012), pp. 289–295

S.E. Smith, D.J. Read Mycorrhizal Symbiosis Academic Press, San Diego, CA (2008)

F.A. Smith, S.E. Smith Structural diversity in (vesicular)-arbuscular mycorrhizal symbioses New Phytol., 137 (1997), pp. 373–388

N. Tang, C.H. San, S. Roy, G. Bécard, B. Zhao, C. Roux A survey of the gene repertoire of Gigaspora rosea unravels conserved features among Glomeromycota for obligate biotrophy Front Microbiol., 1 (2016), p. 233

Y. Tasaki, Y. Kamiya, A. Azwan, T. Hara, T. Joh Gene expression during Pi deficiency in Pholiota nameko: accumulation of mRNAs for two transporters Biosci. Biotechnol. Biochem., 66 (2002), pp. 790–800

J.M. Thevelein Regulation of trehalose metabolism and its relevance to cell growth and function R. Brambl, G.A. Marzluf (Eds.), The Mycota III, Biochemistry and Molecular Biology, Springer-Verlag, Heidelberg (1996), pp. 395–414

B.D. Thomson, D.T. Clarkson, P. Brain Kinetics of phosphorus uptake by the germ-tubes of the vesicular-arbuscular mycorrhizal fungus, Gigaspora margarita New Phytol., 116 (1990), pp. 647–653

S. Timonen, F.A. Smith, S.E. Smith Microtubules of the mycorrhizal fungus Glomus intraradices in symbiosis with tomato roots Can J. Bot., 79 (2001), pp. 307–313

E. Tisserant, A. Kohler, P. Dozolme-Seddas, R. Balestrini, K. Benabdellah, A. Colard, D. Croll, C. Da Silva, S.K. Gomez, R. Koul, et al. The transcriptome of the arbuscular mycorrhizal fungus Glomus intraradices (DAOM 197198) reveals functional tradeoffs in an obligate symbiont New Phytol., 193 (2012), pp. 755–769

E. Tisserant, M. Malbreil, A. Kuoc, A. Kohler, A. Symeonidi, R. Balestrini, P. Charron, N. Duensing, N. Frei dit Frey, V. Gianinazzi-Pearson, et al. Genome of an arbuscular mycorrhizal fungus provides insight into the oldest plant symbiosis Proc. Natl. Acad. Sci. USA, 110 (2013), pp. 20117–20122

A. Trouvelot Mesure du taux de mycorhization VA d'un systeme radiculaire. Recherche de methodes d'estimation ayant une signification fonctionnelle V. Gianinazzi-Pearson, S. Gianinazzi (Eds.), Mycorrhizae: Physiology and Genetics, Institut geNational de la Recherche Agronomique, Paris (1986), pp. 217–221

Y. Uetake, T. Kojima, T. Ezawa, M. Saito Extensive tubular vacuole system in an arbuscular mycorrhizal fungus, Gigaspora margarita New Phytol., 154 (2002), pp. 761–768

M.G.A. van der Heijden, J.N. Klironomos, M. Ursic, P. Moutoglis, R. Streitwolf-Engel, T. Boller, A. Wiemken, I.R. Sanders Mycorrhizal fungal diversity determines plant biodiversity, ecosystem variability and productivity Nature, 396 (1998), pp. 69–72

R. Wild, R. Gerasimaite, J.Y. Jung, V. Truffault, I. Pavlovic, A. Schmidt, A. Saiardi, H.J. Jessen, Y. Poirier, M. Hothorn, et al. Control of eukaryotic phosphate homeostasis by inositol polyphosphate sensor domains Science, 352 (2016), pp. 986–990

D.D. Wykoff, A.H. Rizvi, J.M. Raser, B. Margolin, E.K. O'Shea Positive feedback regulates switching of phosphate transporters in S. cerevisiae Mol. Cell, 27 (2007), pp. 1005–1013

X. Xie, W. Huang, F. Liu, N. Tang, Y. Liu, H. Lin, B. Zhao Functional analysis of the novel mycorrhiza-specific phosphate transporter AsPT1 and PHT1 family from Astragalus sinicus during the arbuscular mycorrhizal symbiosis New Phytol., 198 (2013), pp. 836–852

V. Yadav, M. Kumar, D.K. Deep, H. Kumar, R. Sharma, T. Tripathi, N. Tuteja, A.K. Saxena, A.K. Johri A phosphate transporter from the root endophytic fungus Piriformospora indica plays a role in the phosphate transport to the host plant J. Biol. Chem., 285 (2010), pp. 26532–26544

S. Yang, M. Grønlund, I. Jakobsen, M.S. Grotemeyer, D. Rentsch, A. Miyao, H. Hirochik, C.S. Kumar, V. Sundaresan, N. Salamin Nonredundant regulation of rice arbuscular mycorrhizal symbiosis by two members of the PHOSPHATE TRANSPORTER1 gene family Plant Cell, 24 (2012), pp. 4236–4251

A. Zézé, H. Dulieu, V. Gianinazzi-Pearson DNA cloning and screening of a partial genomic library from an arbuscular mycorrhizal fungus, Scutellospora castanea Mycorrhiza, 4 (1994), pp. 251–254

Q. Zhang, L.A. Blaylock, M.J. Harrison Two Medicago truncatula half-ABC transporters are essential for arbuscule development in arbuscular mycorrhizal symbiosis Plant Cell, 22 (2010), pp. 1483–1497

B. Zhao, A. Trouvelot, S. Gianinazzi, V. Gianinazzi-Pearson Influence of two legume species on hyphal production and activity of two arbuscular mycorrhizal fungi Mycorrhiza, 7 (1997), pp. 179–185

J. Zhu, M.Q. Zhang SCPD: a promoter database of the yeast Saccharomyces cerevisiae Bioinformatics., 15 (1999), pp. 607–611